

1 **Role of endopeptidases in peptidoglycan synthesis mediated by alternative cross-linking**  
2 **enzymes in *Escherichia coli***

3 Henri Voedts<sup>a</sup>, Delphine Dorchêne<sup>a</sup>, Adam Lodge<sup>b#</sup>, Waldemar Vollmer<sup>b</sup>, Michel Arthur<sup>a\*</sup>, Jean-  
4 Emmanuel Hugonnet<sup>a\*</sup>

5 <sup>a</sup> Centre de Recherche des Cordeliers, Sorbonne Université, Inserm, Université de Paris, F-75006  
6 Paris, France; <sup>b</sup> Centre for Bacterial Cell Biology, Biosciences Institute, Newcastle University,  
7 Newcastle Upon Tyne, UK; <sup>#</sup> Present address: Iksuda Therapeutics, The Biosphere, Draymans Way,  
8 Newcastle Helix, Newcastle upon Tyne, NE4 5BX, UK.

9 \* Corresponding authors, [michel.arthur@crc.jussieu.fr](mailto:michel.arthur@crc.jussieu.fr); [jean-emmanuel.hugonnet@crc.jussieu.fr](mailto:jean-emmanuel.hugonnet@crc.jussieu.fr)

10

11 **ABSTRACT**

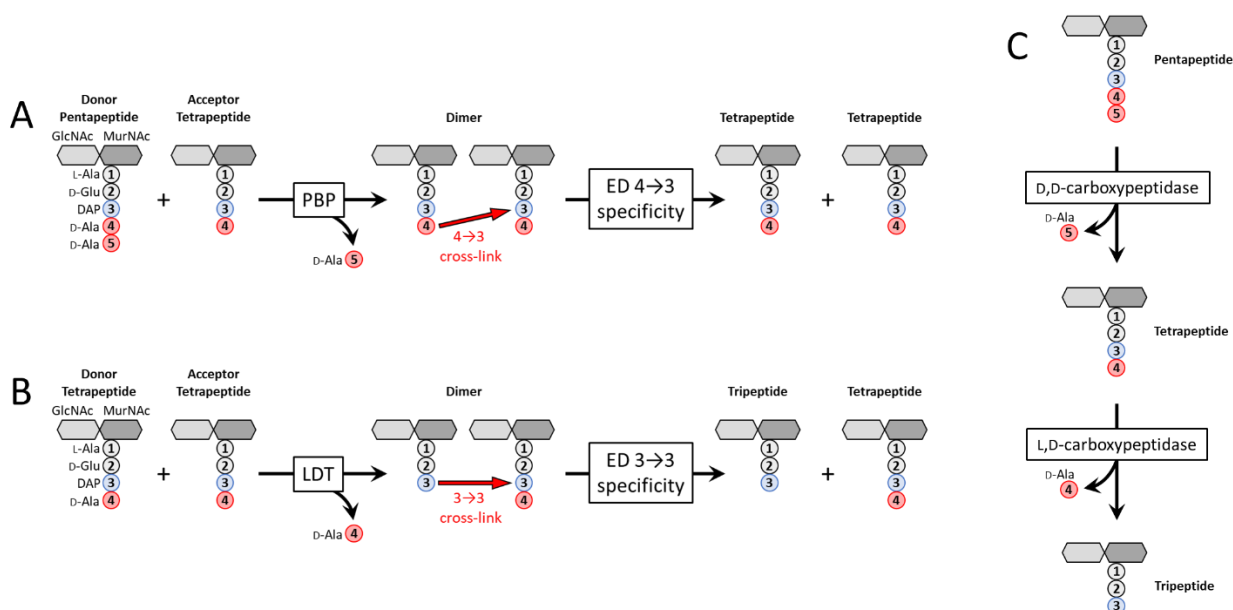
12 Bacteria resist to the turgor pressure of the cytoplasm through a net-like macromolecule, the  
13 peptidoglycan, made of glycan strands connected via peptides cross-linked by penicillin-binding  
14 proteins (PBPs). We recently reported the emergence of  $\beta$ -lactam resistance resulting from a  
15 bypass of PBPs by the YcbB  $L,D$ -transpeptidase (LtdD), which form chemically distinct 3 $\rightarrow$ 3 cross-  
16 links compared to 4 $\rightarrow$ 3 formed by PBPs. Here we show that peptidoglycan expansion requires  
17 controlled hydrolysis of cross-links and identify amongst eight endopeptidase paralogues the  
18 minimum enzyme complements essential for bacterial growth with 4 $\rightarrow$ 3 (MepM) and 3 $\rightarrow$ 3  
19 (MepM and MepK) cross-links. Purified Mep endopeptidases unexpectedly displayed a 4 $\rightarrow$ 3 and  
20 3 $\rightarrow$ 3 dual specificity implying recognition of a common motif in the two cross-link types.  
21 Uncoupling of the polymerization of glycan chains from the 4 $\rightarrow$ 3 cross-linking reaction was found  
22 to facilitate the bypass of PBPs by YcbB. These results illustrate the plasticity of the peptidoglycan  
23 polymerization machinery in response to the selective pressure of  $\beta$ -lactams.

24

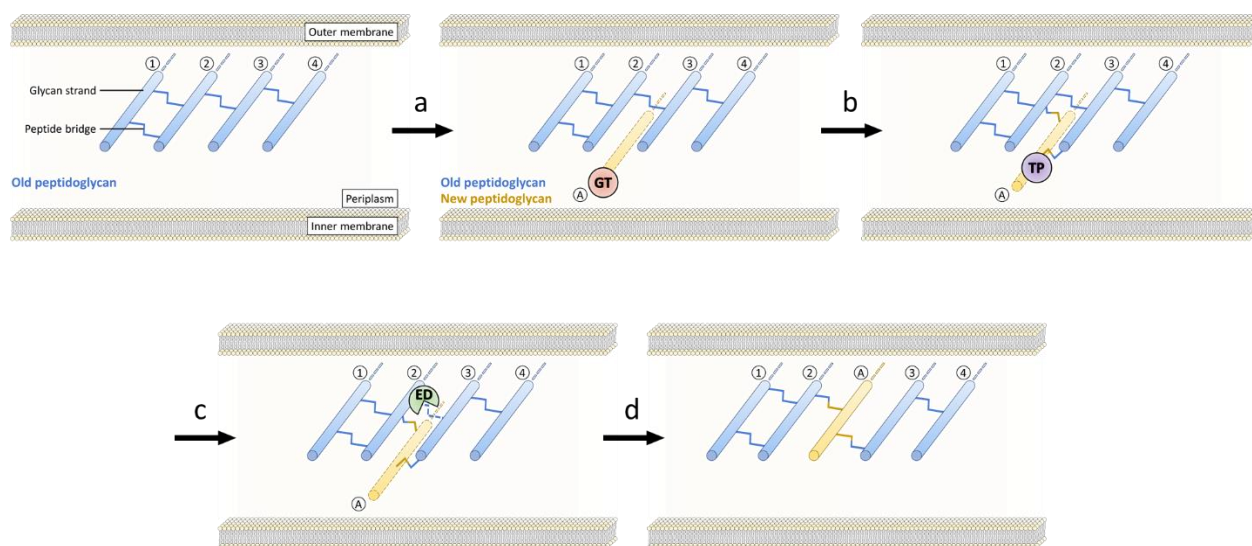
## 25 INTRODUCTION

26 Peptidoglycan (PG) is an essential macromolecule that surrounds the bacterial cell providing  
27 resistance to the osmotic pressure of the cytoplasm and determining cell shape (Turner et al.,  
28 2014). PG is assembled from a disaccharide-peptide subunit consisting of *N*-acetylglucosamine  
29 (GlcNAc) and *N*-acetylmuramic acid (MurNAc) substituted by a stem pentapeptide (L-Ala<sup>1</sup>-γ-D-  
30 Glu<sup>2</sup>-DAP<sup>3</sup>-D-Ala<sup>4</sup>-D-Ala<sup>5</sup> in which DAP is diaminopimelic acid) (Fig. 1A). The subunit is assembled  
31 by glycosyltransferases that polymerize glycan strands and transpeptidases that form amide  
32 bonds between stem peptides carried by adjacent glycan strands. *Escherichia coli* relies on two  
33 types of transpeptidases for the latter reaction (Magnet et al., 2008). The D,D-transpeptidases,  
34 also referred to as penicillin-binding proteins (PBPs), form the most abundant cross-links, which  
35 connect the fourth residue (D-Ala<sup>4</sup>) of an acyl donor to the third residue (DAP<sup>3</sup>) of an acyl acceptor  
36 (4→3 cross-link) (Fig. 1A). The L,D-transpeptidases (LDTs) form 3→3 cross-links that connect two  
37 DAP residues (Fig. 1B). The D-Ala at the 5<sup>th</sup> and 4<sup>th</sup> positions of stem peptides that do not  
38 participate in cross-link formation as donors are fully and partially trimmed by carboxypeptidases  
39 of the D,D and L,D specificities, respectively (Fig. 1C). PBPs and LDTs are structurally unrelated, rely  
40 on different catalytic nucleophiles (Ser *versus* Cys, respectively), and use different acyl donor  
41 stems (pentapeptide *versus* tetrapeptide, respectively) (Mainardi et al., 2008; Sauvage et al.,  
42 2008). PBPs and LDTs also differ by their inhibition profiles since PBPs are potentially inhibited by  
43 all classes of β-lactams (including penams, cepheps, monobactams, and carbapenems) whereas  
44 LDTs are effectively inhibited only by carbapenems (Mainardi et al., 2005). LDTs are fully  
45 dispensable for growth of *E. coli*, at least in laboratory conditions, and form a minority of the  
46 cross-links during exponential growth (6% of the total cross-links) (Glauner et al., 1988; Sanders  
47 and Pavelka, 2013). The proportion of 3→3 cross-links is higher in the stationary phase (Pisabarro  
48 et al., 1985) and in cells experiencing outer membrane assembly stress (Morè et al., 2019). By-  
49 pass of PBPs by LDTs leads to high-level resistance to β-lactams of the penam (such as ampicillin),  
50 cephem (ceftriaxone), and monobactam (aztreonam) classes in engineered *E. coli* strains that  
51 overproduce the YcbB L,D-transpeptidase, also referred to as LdtD, and the guanosine penta- and  
52 tetra-phosphate [(p)ppGpp] alarmones (Hugonnet et al., 2016). PG of such strains grown in the

53 presence of  $\beta$ -lactams exclusively contains 3 $\rightarrow$ 3 cross-links, indicating that the D,D-transpeptidase  
 54 activity of PBPs is fully replaced by the L,D-transpeptidase activity of LDTs.



55  
 56 **Figure 1. Metabolism of PG cross-links and maturation of free stem peptides.** Formation and hydrolysis  
 57 of (A) 4 $\rightarrow$ 3 and (B) 3 $\rightarrow$ 3 crosslinks. The disaccharide-pentapeptide unit is assembled from *N*-  
 58 acetylglucosamine (GlcNAc), *N*-acetylmuramic acid (MurNAc), and five amino acids including *meso*-  
 59 diaminopimelic acid (DAP), which is linked via its L (S) center to the  $\gamma$ -carboxyl group of D-Glu. (C) Hydrolysis  
 60 of the D-Ala<sup>4</sup>-D-Ala<sup>5</sup> and DAP<sup>3</sup>-D-Ala<sup>4</sup> peptide bonds by carboxypeptidases of D,D and L,D specificities,  
 61 respectively.



62  
 63 **Figure S1. Insertion of PG subunits into the growing PG network.** According to this model, one glycan  
 64 strand (A) is polymerized by glycosyltransferases (GTs; step a) and attached to the pre-existing polymer  
 65 (strands 2 and 3) by transpeptidases (TPs; step b). Hydrolysis of the cross-links connecting strands 2 and 3  
 66 by endopeptidases (EDs; step c) results in the expansion of the PG layer (step d). Of note, this model, which

67 applies to the synthesis of the lateral wall, accounts for incorporation of new subunits sheltered from the  
68 cytoplasm osmotic pressure.

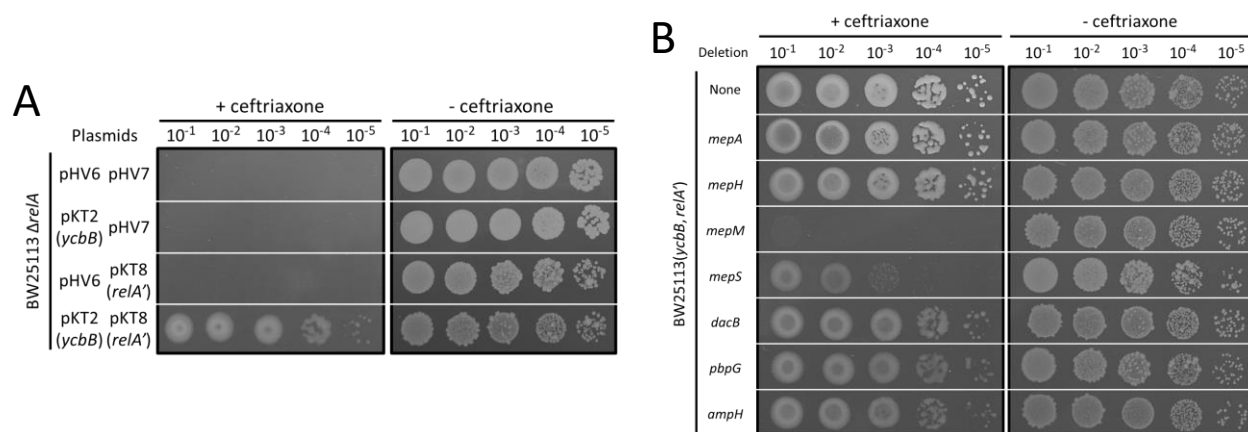
69 Expansion of PG is thought to require highly regulated hydrolytic activities that spatially  
70 control the insertion of new subunits into the growing network of cross-linked glycan strands  
71 (Singh et al., 2012; Vollmer, 2012). Due to the covalent net-like structure of PG, endopeptidases  
72 are predicted to be required for insertion of new subunits leading to the expansion of the PG layer  
73 (supplementary Fig. S1) (Höltje and Heidrich, 2001). The *E. coli* genome encodes eight  
74 endopeptidase paralogues that belong to five enzyme families (Chodisetti and Reddy, 2019; Pazos  
75 and Peters, 2019; Singh et al., 2012). PBP4, PBP7, and AmpH belong to the acyl-serine transferase  
76 superfamily, which also comprises D,D-transpeptidases and D,D-carboxypeptidases. Members of  
77 this superfamily are inhibited by  $\beta$ -lactam antibiotics. The NlpC/P60 cysteine peptidase family  
78 comprises two paralogues (MepH and MepS). Metallo-enzymes are represented by three enzyme  
79 families, LAS metallopeptidases, lysostaphin/M23 peptidases, and M15 peptidases, each  
80 contributing one paralogue (MepA, MepM, and MepK, respectively). The specificity of these eight  
81 paralogues as endopeptidases or carboxypeptidases (Fig. 1) has been explored by using sacculi or  
82 purified PG fragments as substrates (Chodisetti and Reddy, 2019; Engel et al., 1992; Gonzalez-  
83 Leiza et al., 2011; Keck and Schwarz, 1979; Korat et al., 1991; Romeis and Holtje, 1994; Singh et  
84 al., 2012). PBP4, PBP7, AmpH, MepH, and MepS hydrolyze 4 $\rightarrow$ 3 cross-links but PG dimers  
85 containing 3 $\rightarrow$ 3 cross-links were not tested. In contrast, MepA, MepM, and MepK were fully  
86 characterized revealing that MepA hydrolyzes both 4 $\rightarrow$ 3 and 3 $\rightarrow$ 3 cross-links, MepM is specific  
87 to 4 $\rightarrow$ 3 cross-links, and MepK displays a marked preference for 3 $\rightarrow$ 3 cross-links. The  
88 endopeptidases of *E. coli* are redundant and their essential roles can only be revealed by  
89 introducing multiple chromosomal deletions. One study unambiguously showed that hydrolysis  
90 of 4 $\rightarrow$ 3 cross-links by endopeptidases is essential as the triple deletion of genes encoding MepH,  
91 MepM, and MepS was not compatible with growth of *E. coli* in laboratory conditions (Singh et al.,  
92 2012; comment by Vollmer, 2012). Several endopeptidases interact genetically and physically  
93 with the outer membrane anchored adaptor protein NlpI supporting overlapping functions during  
94 the cell cycle (Banzhaf et al., 2020).

95           The dual capacity of *E. coli* to use transpeptidases of the D,D and L,D specificities raises the  
96 possibility that polymerization of PG containing 4→3 or 3→3 cross-links involves two overlapping  
97 sets of endopeptidases. To address this question, we used an *E. coli* strain that conditionally and  
98 exclusively relies on the formation of 3→3 cross-links for growth in the presence of ampicillin or  
99 ceftriaxone (Hugonnet et al., 2016). By introducing serial deletions of endopeptidase genes, we  
100 showed that the 4→3 and 3→3 modes of PG polymerization both require hydrolysis of cross-links.  
101 We identified distinct sets of endopeptidases that are essential for growth involving the two  
102 modes of PG cross-linking. Strikingly, impaired digestion of nascent glycan strands by a lytic  
103 transglycosylase was found to favor PG polymerization mediated by LDTs. These results highlight  
104 the functional plasticity of PG polymerization complexes to accommodate various PG cross-linking  
105 enzymes and hydrolases.

106 **RESULTS**

107 **MepM is essential for  $\beta$ -lactam resistance mediated by the YcbB L,D-transpeptidase**

108 The role of endopeptidases was assessed in *E. coli* BW25113  $\Delta$ *relA* pKT2(*ycbB*) pKT8(*relA'*),  
109 BW25113(*ycbB*, *relA'*) in short, which enables controlling the relative contribution of formation  
110 of 4 $\rightarrow$ 3 and 3 $\rightarrow$ 3 cross-links to PG polymerization (Hugonnet et al., 2016). In this strain, the *ycbB*  
111 L,D-transpeptidase gene carried by plasmid pKT2 is expressed under the control of an IPTG-  
112 inducible promoter. Plasmid pKT8 carries an L-arabinose-inducible copy of the *relA'* gene  
113 encoding a truncated version of RelA (residues 1 to 455), which synthesizes the (p)ppGpp  
114 alarmone in an unregulated manner due to the absence of the C-terminal ribosome binding  
115 module (Schreiber et al., 1991). In the presence of both inducers, production of YcbB and RelA' is  
116 sufficient for full bypass of the D,D-transpeptidase activity of PBPs by the L,D-transpeptidase  
117 activity of YcbB (Fig. 2A). This enables bacterial growth in the presence of ampicillin or ceftriaxone  
118 since these drugs do not inhibit the YcbB L,D-transpeptidase. Testing for the inducible expression  
119 of  $\beta$ -lactam resistance in BW25113(*ycbB*, *relA'*) therefore provides a means to identify genes that  
120 are essential for growth when PG cross-linking is exclusively mediated by the YcbB L,D-  
121 transpeptidase. We used this phenotypic assay to assess the individual role of seven of the eight  
122 endopeptidases of *E. coli* following single-gene deletions in the BW25113(*ycbB*, *relA'*) strain (Fig.  
123 2B). The remaining endopeptidase MepK could not be tested by this approach since deletion of  
124 the corresponding gene was not compatible with the presence of plasmid pKT2(*ycbB*) (see below).  
125 Mutants with deletion of *mepA*, *mepH*, *dacB*, *pbpG*, or *ampH* were resistant to ceftriaxone.  
126 Deletion of *mepS* decreased plating efficiency in the presence of the drug. Deletion of *mepM*  
127 abolished expression of  $\beta$ -lactam resistance. These results are surprising since MepM and MepS  
128 were not reported to hydrolyze 3 $\rightarrow$ 3 cross-links (Chodiseti and Reddy, 2019; Singh et al., 2012).



129  
 130 **Figure 2. MepM is essential for YcbB-mediated  $\beta$ -lactam resistance.** Growth was tested in the presence  
 131 of ceftriaxone at 8  $\mu$ g/ml (+ ceftriaxone) or in the absence of the drug (- ceftriaxone) on BHI agar plates  
 132 supplemented with 40  $\mu$ M IPTG and 1% L-arabinose for induction of *ycbB* and *relA'*, respectively. (A)  
 133 BW25113  $\Delta$ *relA* derivatives harboring plasmids pKT2(*ycbB*), pKT8(*relA'*) and the vectors pHV6 and pHV7  
 134 used to construct these plasmids, respectively. Expression of  $\beta$ -lactam resistance requires induction of  
 135 both *ycbB* and *relA'*. (B) BW25113(*ycbB*, *relA'*) and its derivatives obtained by individual deletion of  
 136 endopeptidase genes. BW25113(*ycbB*, *relA'*) is an abbreviated name for BW25113  $\Delta$ *relA* pKT2(*ycbB*)  
 137 pKT8(*relA'*).

138  
 139 **Production of YcbB is lethal in the absence of MepK**

140 The gene encoding MepK, an endopeptidase with the dual 4 $\rightarrow$ 3 and 3 $\rightarrow$ 3 specificities was readily  
 141 deleted from the chromosome of BW25113  $\Delta$ *relA*. The resulting strain, BW25113  $\Delta$ *relA*  $\Delta$ *mepK*  
 142 was transformed with pKT2(*ycbB*), pKT8(*relA'*), or both plasmids in combination (co-  
 143 transformation). Tetracycline and chloramphenicol were used to select transformants that  
 144 acquired pKT2(*ycbB*) and pKT8(*relA'*), respectively. Plasmid pKT8(*relA'*) was readily introduced  
 145 into BW25113  $\Delta$ *relA*  $\Delta$ *mepK* by transformation ( $10^8$  transformants per  $\mu$ g of DNA). Plasmid  
 146 pKT2(*ycbB*) alone or in combination with pKT8(*relA'*) could not be introduced into BW25113  $\Delta$ *relA*  
 147  $\Delta$ *mepK* (< 5 transformants per  $\mu$ g of DNA). The same plating efficacies were observed in selective  
 148 media containing IPTG, L-arabinose, or both inducers, in addition to tetracycline and  
 149 chloramphenicol. These results show that production of the YcbB L,D-transpeptidase is lethal in  
 150 the absence of MepK, in agreement with a recent report (Chodiseti and Reddy, 2019). Thus,  
 151 cleavage of 3 $\rightarrow$ 3 cross-links by MepK is essential for bacterial growth when the proportion of 3 $\rightarrow$ 3  
 152 cross-links is increased in the presence of a plasmid copy of *ycbB*. Quantitatively, the basal level  
 153 of *ycbB* expression in the absence of IPTG was sufficient for the lethal phenotype associated with



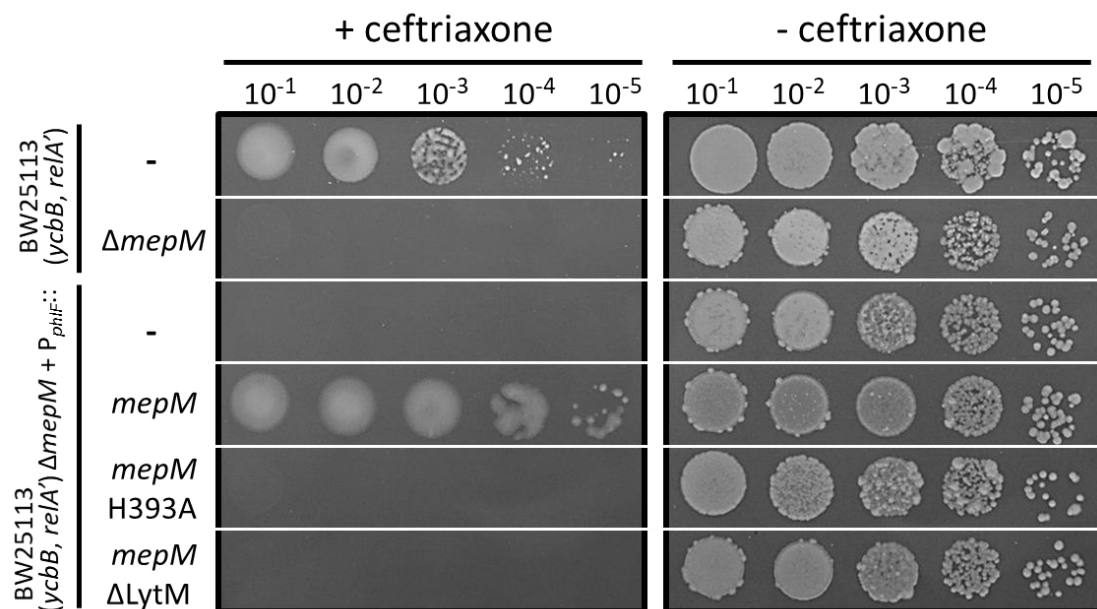
154 the *mepK* deletion. Under non-inducing conditions the relative proportion of 4→3 and 3→3 cross-  
155 links in the PG extracted from exponential phase cultures of BW25113(*ycbB*, *relA'*) was in the  
156 order of 60% and 40%, respectively (data not shown). Thus, the cleavage of 3→3 cross-links by  
157 MepK was essential even if these cross-links co-existed with 4→3 cross-links formed by the PBPs.

158

### 159 **The hydrolytic activity of MepM is essential for $\beta$ -lactam resistance**

160 Deletion of the *mepM* gene abolished YcbB-mediated  $\beta$ -lactam resistance (above, Fig. 2B) even  
161 though this endopeptidase was not reported to cleave 3→3 cross-links (Chodisetti and Reddy,  
162 2019; Singh et al., 2012). We therefore considered the possibility that the essential role of *mepM*  
163 in resistance could involve an as yet unknown function in addition to its 4→3-endopeptidase  
164 activity. MepM (440 residues) comprises a LytM (lysostaphin/M23 peptidase) domain and a LysM  
165 PG-binding domain (Pfam: P0AFS9). Complementation analysis of the *mepM* deletion in  
166 BW25113(*ycbB*, *relA'*) was performed with plasmids encoding (i) MepM, (ii) MepM H<sup>393</sup>A  
167 harboring an Ala residue at position 393 in place of an essential catalytic His residue conserved in  
168 members of the M23 peptidase family, and (iii) MepM  $\Delta$ LytM lacking the C-terminal  
169 endopeptidase catalytic domain (Fig. 3). Expression of  $\beta$ -lactam resistance by BW25113(*ycbB*,  
170 *relA'*)  $\Delta$ *mepM* was only restored by the plasmid harboring an intact copy of the *mepM* gene. Thus,  
171 the complementation analysis led to the conclusion that the endopeptidase activity of MepM is  
172 essential for YcbB-mediated resistance to  $\beta$ -lactams.





173

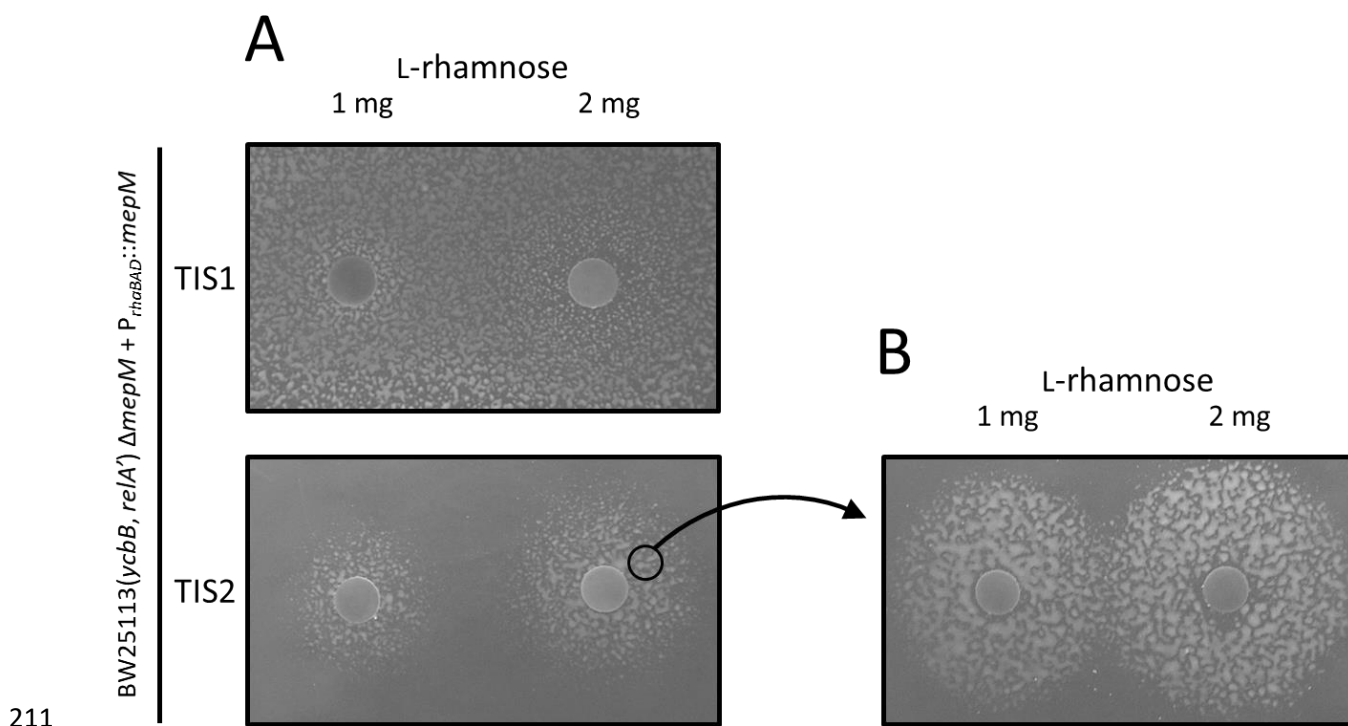
174 **Figure 3. MepM endopeptidase activity is required for YcbB-mediated  $\beta$ -lactam resistance.** Growth of  
 175 BW25113(*ycbB*, *relA'*), BW25113(*ycbB*, *relA'*)  $\Delta mepM$ , and its derivatives harboring plasmids encoding  
 176 MepM, MepM H<sup>393A</sup>, and MepM  $\Delta LytM$  were tested in the presence of ceftriaxone at 8  $\mu$ g/ml (+  
 177 ceftriaxone) or in the absence of the drug (- ceftriaxone) in BHI agar plates supplemented with 40  $\mu$ M IPTG  
 178 and 1% L-arabinose for induction of *ycbB* and *relA'*, respectively. The genes encoding MepM, MepM H<sup>393A</sup>,  
 179 and MepM  $\Delta LytM$  were inserted into the vector pHV9 under the control of the P<sub>phIF</sub> promoter, which is  
 180 inducible by 2,4-diacetylphloroglucinol (DAPG). Basal level of expression of *mepM* under the control of  
 181 P<sub>phIF</sub> was sufficient to restore ceftriaxone resistance in the absence of the inducer.

182

183 **The essential role of the endopeptidase activity of MepM in  $\beta$ -lactam resistance is not restricted**  
 184 **to the transition from 4 $\rightarrow$ 3 to 3 $\rightarrow$ 3 cross-links triggered by the induction of *ycbB* and *relA'***

185 The experiment reported above did not rule out the possibility that hydrolysis of 4 $\rightarrow$ 3 cross-links  
 186 by MepM might be transiently essential to enable bypass of PBPs by YcbB, *i.e.* cleavage of 4 $\rightarrow$ 3  
 187 cross-links by MepM could be initially essential to enable insertion of new PG subunits into the  
 188 PG network by YcbB. Ultimately, this would lead to replacement of 4 $\rightarrow$ 3 by 3 $\rightarrow$ 3 cross-links and  
 189 could then suppress the essential role of 4 $\rightarrow$ 3 cross-link cleavage by MepM. According to this  
 190 hypothesis, MepM would only be essential during the transition between the two modes of PG  
 191 cross-linking. To test this possibility, we sought a plasmid construct enabling tight regulation of  
 192 the *mepM* gene. In a first attempt, *mepM* was cloned under the control of the L-rhamnose-  
 193 inducible promoter (P<sub>rhaBAD</sub>) of the pHV30 vector. Complementation of the *mepM* deletion of  
 194 BW25113(*ycbB*, *relA'*) was obtained both in the presence or absence of L-rhamnose indicating

195 that the un-induced level of *ycbB* afforded by this plasmid construct was too high (Fig. 4A). To  
196 address this issue, the level of *mepM* expression was reduced by replacing the sequence  
197 containing the translation initiation signal (TIS1) of *mepM* by a weaker translation initiation signal  
198 (TIS2). TIS1 (aAAGAGGAGAAAtgacataATG) combined an ATG initiation codon to a “strong”  
199 ribosome-binding-site (RBS) with extensive complementarity (underlined) to the 3’ OH extremity  
200 of 16S rRNA (5’- AUCACCUCCUUA-3’OH) (Elowitz and Leibler, 2000). TIS2 (acacAGGAcacttaTTG)  
201 combined a TTG initiation codon to an RBS with limited complementarity to 16S rRNA (5’-  
202 AUCACCUCCUUA-3’OH) (Hecht et al., 2017; Ringquist et al., 1992; Vellanoweth and Rabinowitz,  
203 1992). In contrast to the results obtained with TIS1, the presence of L-rhamnose was required for  
204  $\beta$ -lactam resistance if *mepM* was expressed under the control of TIS2 (Fig. 4A). L-rhamnose  
205 requirement for growth in the presence of ceftriaxone was not abolished by pre-exposure to the  
206 inducer (Fig. 4B). These results indicate that the essential role of MepM in  $\beta$ -lactam resistance is  
207 not limited to the transition between the two modes of PG cross-linking, *i.e.* from 4 $\rightarrow$ 3 to 3 $\rightarrow$ 3.  
208 Since all D,D-transpeptidases are inhibited by ceftriaxone, these results also indicate that the  
209 hydrolytic activity of MepM is essential in conditions in which 4 $\rightarrow$ 3 cross-links are not detectable  
210 (Hugonnet et al., 2016; Kocaoglu and Carlson, 2015).



212 **Figure 4. MepM is essential for  $\beta$ -lactam resistance beyond the transition from 4 $\rightarrow$ 3 to 3 $\rightarrow$ 3 PG cross-**  
213 **linking.** The *mepM* gene was expressed under the control of TIS1 or TIS2 (translation initiation) and of  
214 *P<sub>rhaBAD</sub>* (the L-rhamnose-inducible promoter of vector pHV30). Growth of BW25113(*ycbB*, *relA'*)  $\Delta$ *mepM*  
215 harboring the pHV30 derivatives was tested on BHI agar supplemented with ceftriaxone 8  $\mu$ g/ml, IPTG 40  
216  $\mu$ M (induction of *ycbB*) and L-arabinose 1% (induction of *relA'*). (A) For TIS2, growth around paper disks  
217 containing 1 or 2 mg of L-rhamnose indicated that induction of the expression of *mepM* was required for  
218 ceftriaxone resistance. In contrast, a higher level of translation from TIS1 was sufficient for ceftriaxone  
219 resistance in the absence of the inducer. (B) The experiment was repeated with bacteria pre-exposed to  
220 L-rhamnose that were harvested at the vicinity of the disk containing 2 mg of L-rhamnose. Expression of  
221 ceftriaxone resistance remained dependent on the presence of L-rhamnose indicating that the  
222 requirement for MepM is not transient. The diameter of the growth zones is larger in panel (B) than in  
223 panel (A) as expected from the fact that bacteria in the inoculum used in (B) had been grown in the  
224 presence of the inducer and already contained MepM. In (A) growth is only possible after diffusion of L-  
225 rhamnose in the medium prior to the action of ceftriaxone. At a distance from the disk, diffusion was not  
226 sufficiently rapid to observe resistance.

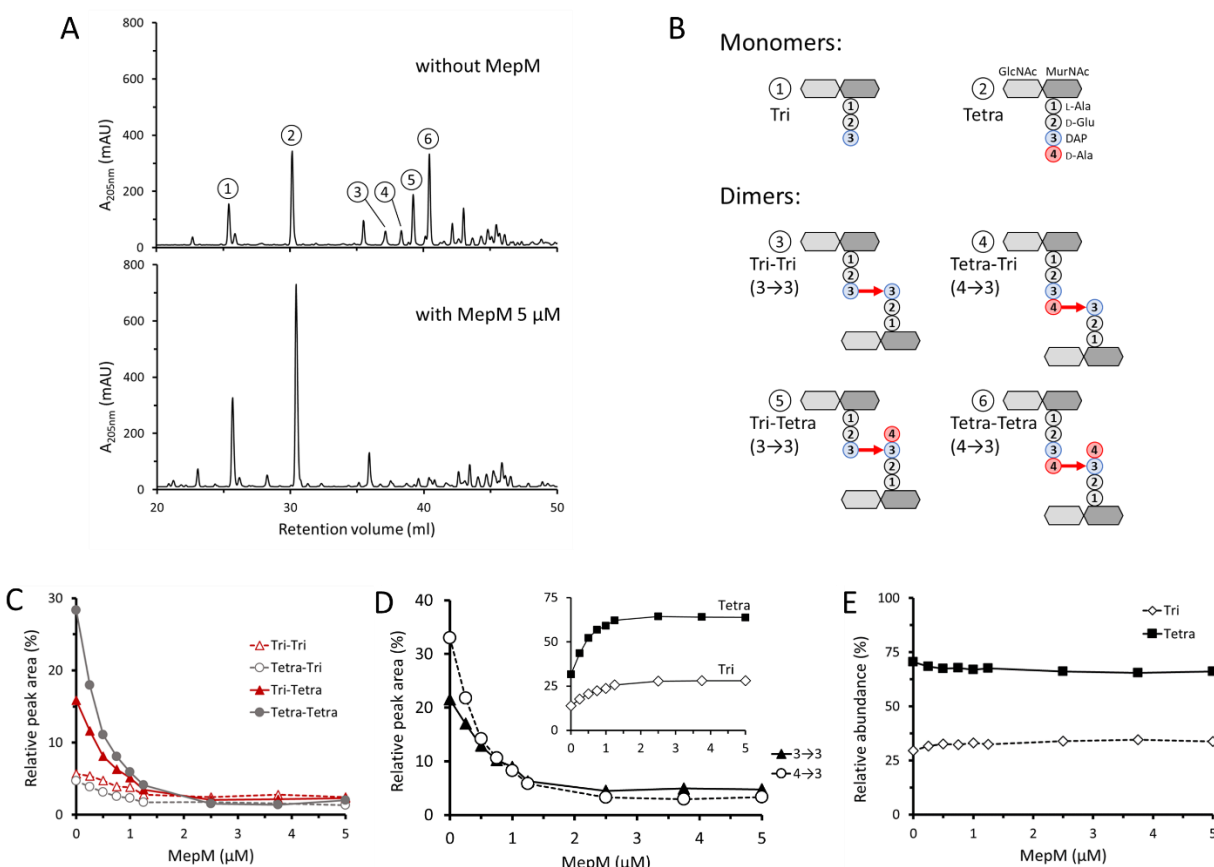
227

#### 228 **MepM hydrolyzes both 4 $\rightarrow$ 3 and 3 $\rightarrow$ 3 cross-links *in vitro***

229 The essential role of the endopeptidase activity of MepM in the context of LDT-mediated PG  
230 cross-linking (above) led us to reconsider the specificity of the enzyme. Previous analyses were  
231 based on incubation of MepM and lysozyme with an *E. coli* PG preparation containing minute  
232 amounts of 3 $\rightarrow$ 3 cross-links (Chodisetti and Reddy, 2019; Singh et al., 2012). Analyses of *rp*HPLC  
233 profiles revealed that the major dimers containing 4 $\rightarrow$ 3 cross-links were digested by MepM but  
234 minor peaks corresponding to dimers containing 3 $\rightarrow$ 3 cross-links remained unchanged in the  
235 presence of the enzyme leading to the conclusion that MepM was specific to 4 $\rightarrow$ 3 cross-links  
236 (Chodisetti and Reddy, 2019; Singh et al., 2012). To improve the sensitivity of the assay, we  
237 purified MepM and reproduced this analysis with a PG preparation of *E. coli* BW25113 grown to  
238 stationary phase in minimal medium, which contained a higher proportion of 3 $\rightarrow$ 3 cross-links (Fig.  
239 5A, upper panel.) The mucopeptides corresponding to the indicated peaks are shown in Fig. 5B  
240 (see supplementary Fig. S2 for determination of the structure of mucopeptides by mass  
241 spectrometry). Full digestion of all dimers was observed upon incubation of this PG preparation  
242 with MepM (5  $\mu$ M) indicating that the endopeptidase hydrolyzes both 4 $\rightarrow$ 3 and 3 $\rightarrow$ 3 cross-links  
243 to completion (Fig. 5A, lower panel). Incubation of the PG preparation with lower concentrations  
244 of MepM led to partial hydrolysis of the dimers (Fig. 5C). Comparison of the relative abundance  
245 of mucopeptides based on the integration of peak areas in the chromatograms showed the  
246 expected increase in monomers upon digestion of dimers (Fig. 5D). The concentrations of MepM

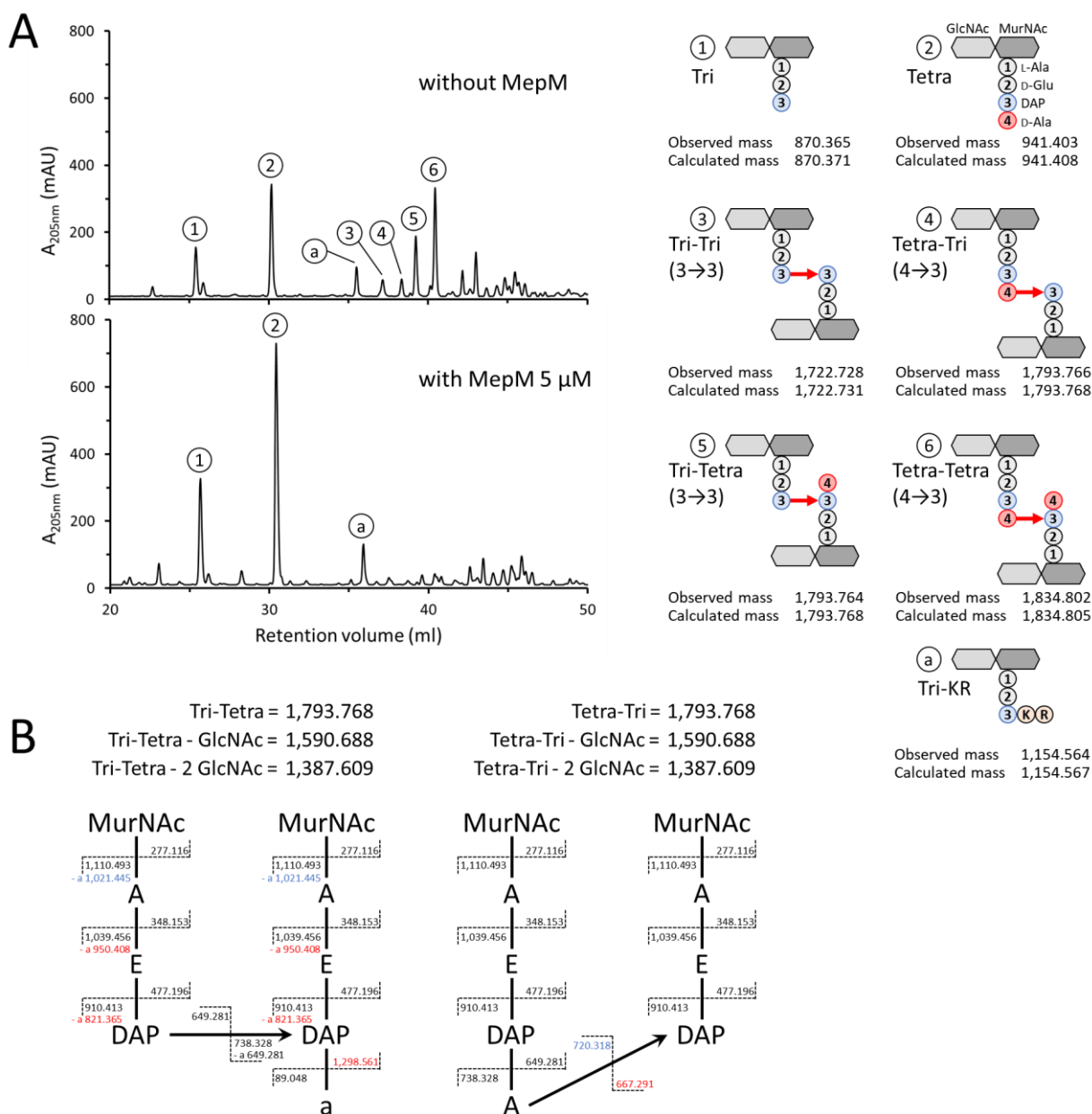
247 required for hydrolysis of half of the muropeptides containing 4→3 and 3→3 cross-links were 0.4  
 248 μM and 0.7 μM, respectively, revealing similar apparent hydrolysis efficacies for the two types of  
 249 cross-links under the assay conditions (Fig. 5D). These results indicate that hydrolysis of 3→3  
 250 cross-links may account for the essential role of MepM in conditions in which the L,D-  
 251 transpeptidase activity of YcbB fully replaces the D,D-transpeptidase activity of the PBPs, as  
 252 inferred from expression of ceftriaxone resistance by BW25113(*ycbB*, *relA'*) but not by its  $\Delta$ *mepM*  
 253 derivative (Fig. 2B).

254 The sum of the relative proportion of tripeptide and tetrapeptide stems in all monomers and  
 255 dimers did not vary upon addition of MepM (Fig. 5E). This observation indicates that MepM did  
 256 not hydrolyze D-Ala<sup>4</sup> from tetrapeptide monomers or from tetrapeptide stems located in the  
 257 acceptor position of dimers. Thus, MepM did not display any L,D-carboxypeptidase activity.



258  
 259 **Figure 5. Hydrolysis of 4→3 and 3→3 cross-links by purified MepM.** (A) *rpHPLC* chromatograms of sacculi  
 260 isolated from BW25113 grown in minimal medium to stationary phase and digested by lysozyme (upper  
 261 panel) or by lysozyme and 5 μM MepM (lower panel). Absorbance was monitored at 205 nm (mAU, milli-  
 262 absorbance unit). (B) Structure of the muropeptides as determined by mass spectrometry (supplementary

263 Fig. S2). (C) Hydrolysis of the four types of dimers by MepM. Sacculi were incubated with lysozyme and  
 264 MepM at various concentrations. The relative abundance of the muuropeptides was estimated by  
 265 calculating the relative peak areas. (D) Hydrolysis of dimers containing 4→3 and 3→3 cross-links by MepM.  
 266 The relative peak areas of Tri-Tri and Tri-Tetra containing 3→3 cross-links and that of Tetra-Tri and Tetra-  
 267 Tetra containing 4→3 cross-links were combined. The inset shows variations in the relative peak areas of  
 268 the Tri and Tetra monomers. (E) Relative abundance of Tri and Tetra stems in all muuropeptides.



269  
 270 **Figure S2.** (A) Mass spectrometry analysis of muuropeptides obtained by digestion of sacculi from BW25113  
 271 with lysozyme (upper panel) or lysozyme plus MepM (lower panel). The observed and calculated  
 272 monoisotopic mass are indicated in Dalton. Peak a corresponds to a disaccharide-tripeptide substituted  
 273 by a Lys-Arg (KR) dipeptide originating from digestion of the covalently-bond Braun lipoprotein by trypsin  
 274 (Magnet et al., 2008). (B) Discrimination of isomers containing 3→3 (Tri-Tetra) and 4→3 (Tetra-Tri) cross-

275 links by tandem mass spectrometry. All fragments lost both GlcNAc molecules. Fragments that are specific  
276 of each isomer are shown in red. Fragments specific of an isomer but which can also be found in the other  
277 isomer following loss of a water molecule are shown in blue. Mass of fragments is shown in Dalton. A, L-  
278 Ala or D-Ala; a, C-terminal D-Ala; E, D-Glu; DAP, diaminopimelic acid.

279  
280 **Design of an assay to investigate the redundancy of endopeptidases required for YcbB-**  
281 **mediated  $\beta$ -lactam resistance**

282 Single deletion of endopeptidase genes revealed four phenotypes (above, Fig. 2B). (i) Deletion of  
283 *mepK* was not compatible with production of YcbB. (ii) Deletion of *mepM* abolished YcbB-  
284 mediated ceftriaxone resistance. (iii) Deletion of *mepS* impaired growth in the presence of  
285 ceftriaxone. (iv) Deletion of *mepA*, *mepH*, *dacB*, *pbpG*, or *ampH* had no impact on growth in the  
286 presence of ceftriaxone. The absence of any phenotypic alteration associated with the individual  
287 deletion of the latter genes does not necessarily imply that the corresponding endopeptidases  
288 are unable to participate in the hydrolysis of 3 $\rightarrow$ 3 cross-links. Indeed, the function of these  
289 enzymes may be redundant. Alternatively, their level of production may be insufficient under the  
290 tested growth conditions. To investigate these possibilities, each of the eight endopeptidase  
291 genes was independently cloned under the control of the “strong” TIS1 translation initiation  
292 signal downstream from the *P<sub>rhaBAD</sub>* promoter of the vector pHV30 in order to modulate the level  
293 of endopeptidase production based on induction by L-rhamnose. The plasmids were introduced  
294 into BW25113(*ycbB*, *relA'*)  $\Delta$ *mepM* and growth of the resulting strains was tested in the presence  
295 or absence of L-rhamnose and in the presence or absence of ceftriaxone in all combinations (Fig.  
296 6).

297  
298 **Overexpression of *mepM* is toxic in the presence of ceftriaxone**

299 The assay described above revealed that the basal level of expression of the plasmid copy of  
300 *mepM* in the absence of the inducer was sufficient to restore growth of BW25113(*ycbB*, *relA'*)  
301  $\Delta$ *mepM* in the presence of ceftriaxone (Fig. 6). Induction of the *mepM* gene by L-rhamnose  
302 prevented growth in the presence of ceftriaxone but not in the absence of the drug. These results  
303 suggest that overproduction of MepM inhibits growth by cleavage of 3 $\rightarrow$ 3 cross-links if 4 $\rightarrow$ 3  
304 cross-links are absent due to the inactivation of the PBPs by ceftriaxone.



305

306 **Overexpression of *mepS* complements the *mepM* deletion for expression of YcbB-mediated  $\beta$ -**  
307 **lactam resistance**

308 MepS restored growth of BW25113(*ycbB*, *relA'*)  $\Delta$ *mepM* only in the presence of the inducer (Fig.  
309 6). Thus, MepM and MepS have overlapping functions although overproduction of MepS was  
310 required to compensate for the absence of MepM. As mentioned above (Fig. 2B), deletion of  
311 *mepS* impaired but did not abolish ceftriaxone resistance in BW25113(*ycbB*, *relA'*). Together these  
312 results indicate that expression of *mepS* in its native chromosomal environment contributes to  
313 resistance but the level of its expression is not sufficient to compensate for the absence of MepM.

314

315 **Partial complementation of the *mepM* deletion by *mepH***

316 The plasmid encoding MepH partially restored growth of BW25113(*ycbB*, *relA'*)  $\Delta$ *mepM* on  
317 ceftriaxone only in the presence of L-rhamnose (Fig. 6). This result indicates that MepH, like MepS,  
318 replaces MepM for the expression of ceftriaxone resistance if MepH is overproduced.

319

320 **Purified MepS and MepH hydrolyze 4 $\rightarrow$ 3 and 3 $\rightarrow$ 3 cross-links (endopeptidase activity) and the**  
321 **DAP-D-Ala bond of tetrapeptide stems (L,D-carboxypeptidase activity)**

322 Complementation of  $\Delta$ *mepM* by overproduction of MepS and MepH prompted us to evaluate the  
323 specificity of these enzymes, as described above for MepM. MepH and MepS both hydrolyzed  
324 4 $\rightarrow$ 3 and 3 $\rightarrow$ 3 cross-links (Fig. 7A and B). MepS showed no preference for 4 $\rightarrow$ 3 or 3 $\rightarrow$ 3 cross-links  
325 while MepH displayed a strong preference for 4 $\rightarrow$ 3 cross-links. The weak hydrolytic activity of  
326 MepH on 3 $\rightarrow$ 3 cross-links may account for the fact that the overproduction of MepH can only  
327 partially compensate for the absence of MepM (Fig. 6, above). Both MepS and MepH displayed  
328 L,D-carboxypeptidase activity leading to rapid conversion of tetrapeptide stems into tripeptide  
329 stems (Fig. 7A and B).

330

331 **MepA and MepK do not compensate the absence of MepM**



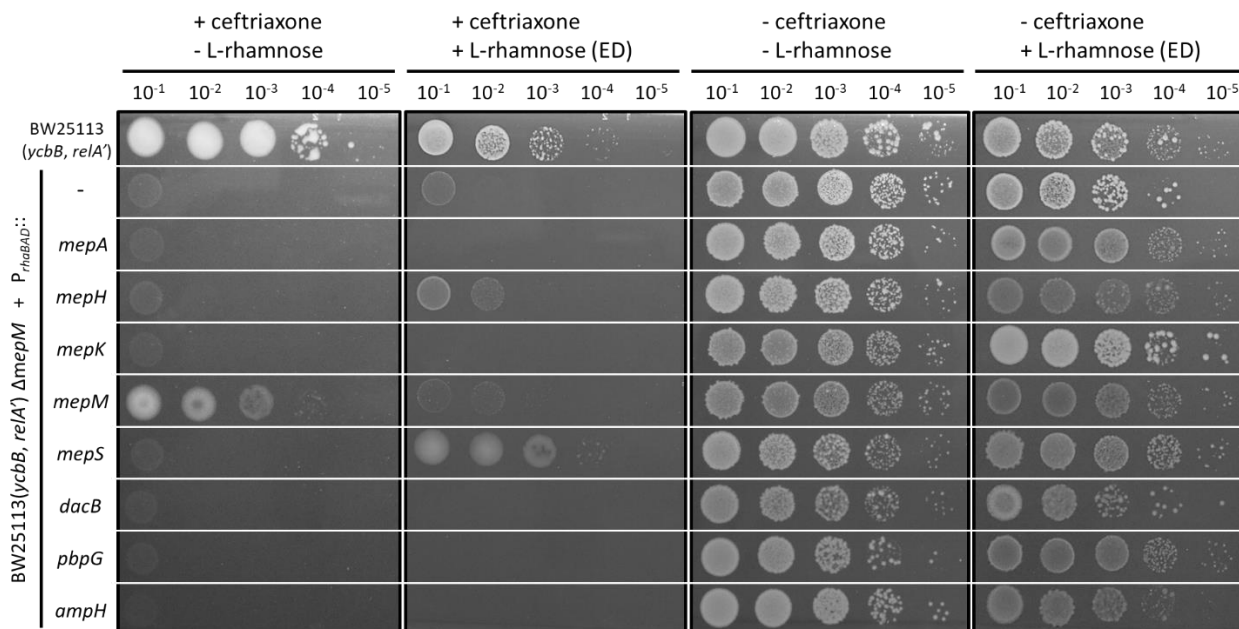
332 In spite of the fact that MepA and MepK were previously shown to cleave 3→3 cross-links  
333 (Chodisetti and Reddy, 2019; Engel et al., 1992), growth of BW25113(*ycbB*, *relA'*)  $\Delta$ *mepM* on  
334 ceftriaxone was not restored by overproduction of these enzymes (Fig. 6). Thus, there was not a  
335 strict correlation between the ability of the endopeptidases to hydrolyze 3→3 cross-links *in vitro*  
336 and their ability to restore growth of BW25113(*ycbB*, *relA'*)  $\Delta$ *mepM*. This absence of correlation  
337 was particularly striking for MepK since this endopeptidase, which preferentially hydrolyze 3→3  
338 cross-links *in vitro* (Chodisetti and Reddy, 2019), did not complement the *mepM* deletion although  
339 it was required for growth of BW25113(*ycbB*, *relA'*) expressing the *ycbB* L,D-transpeptidase gene.

340 These results indicate that functional properties of the endopeptidases, beyond their mere  
341 hydrolytic specificity, are relevant to the bypass of the D,D-transpeptidase activity of PBPs by the  
342 L,D-transpeptidase activity of YcbB. These properties may include the interaction of the  
343 endopeptidases with other proteins that regulate their spatiotemporal activity (see discussion  
344 section).

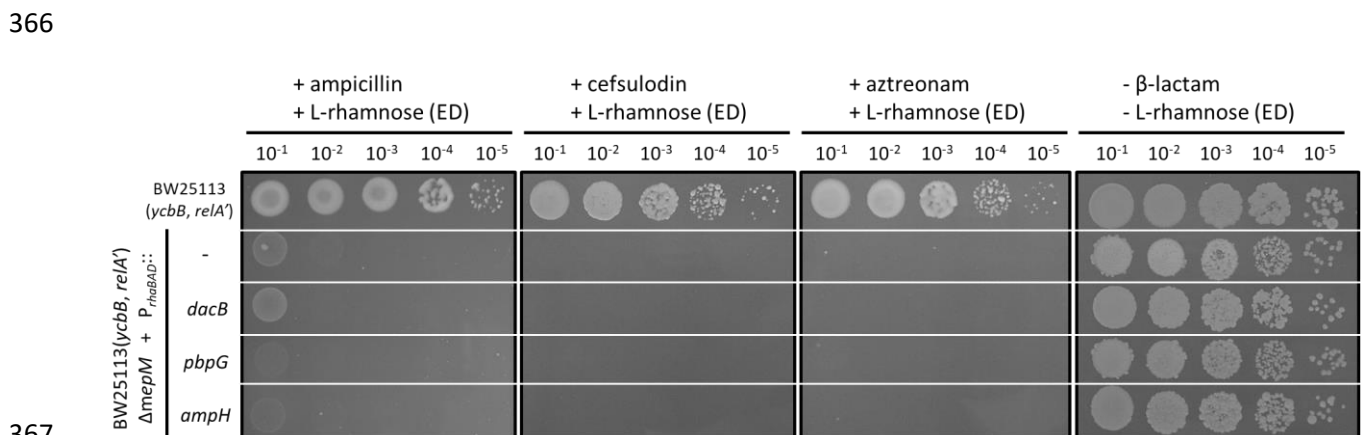
345

#### 346 **Endopeptidases of the PBP family do not compensate the absence of MepM**

347 Complementation of the *mepM* deletion was not observed for PBP4, PBP7, and AmpH both in the  
348 presence or absence of induction of the corresponding genes by L-rhamnose (Fig. 6). There is a  
349 caveat for these endopeptidases since they are potentially inhibited by ceftriaxone. To address  
350 this issue, the complementation test was repeated with ampicillin, cefsulodin, and aztreonam,  
351 which were reported to exhibit different selectivities for inhibition of the PBPs (Henderson et al.,  
352 1997; Kocaoglu and Carlson, 2015). Plasmids encoding PBP4, PBP7, and AmpH did not restore  
353 growth of BW25113(*ycbB*, *relA'*)  $\Delta$ *mepM* in the presence of ampicillin, cefsulodin, and aztreonam  
354 (supplementary Fig. S3) confirming that these endopeptidases are unable to compensate for the  
355 absence of MepM. PBP4 and PBP7 were purified and shown to only cleave 4→3 cross-links (Fig.  
356 7C and D). Thus, the absence of complementation of the *mepM* deletion by the plasmids encoding  
357 these PBPs can be accounted for by their lack of hydrolytic activities on 3→3 cross-linked dimers.  
358 PBP4 and PBP7 did not display L,D-carboxypeptidase activity.

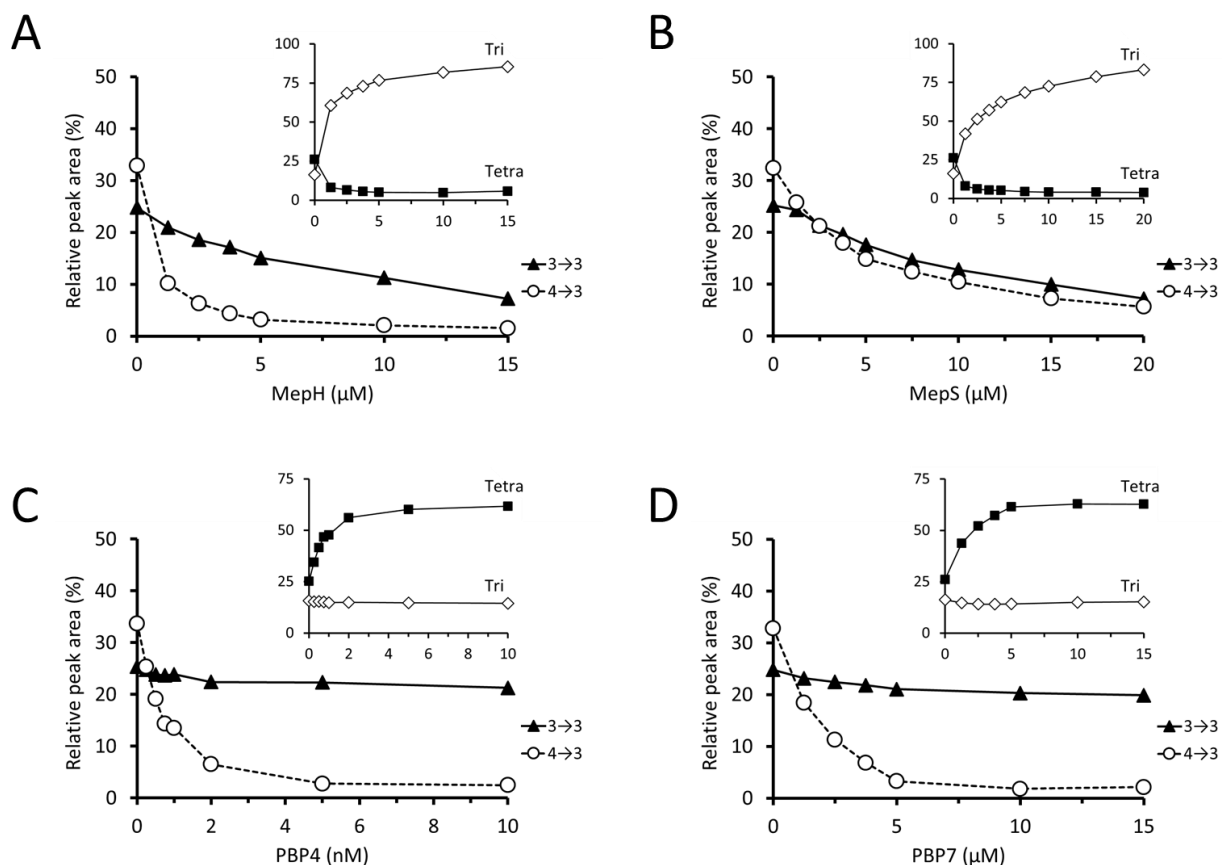


359  
360 **Figure 6. Complementation of the *mepM* deletion by plasmids encoding L-rhamnose-inducible copies of**  
361 **the eight endopeptidase genes.** Functional complementation of the *mepM* deletion in BW25113(*ycbB*,  
362 *relA'*)  $\Delta$ *mepM* was performed with the pHV30 vector or recombinant plasmids encoding each of the eight  
363 endopeptidases under the control of the  $P_{rhaBAD}$  promoter. Induction of endopeptidase (ED) genes was  
364 performed with 0.2% L-rhamnose in the presence or absence of 8  $\mu$ g/ml ceftriaxone. BHI agar plates  
365 contained 40  $\mu$ M IPTG and 1% L-arabinose for induction of *ycbB* and *relA'*, respectively.



367  
368  
369 **Figure S3. Complementation of the *mepM* deletion by endopeptidases of the PBP family.** Functional  
370 complementation of the *mepM* deletion of BW25113(*ycbB*, *relA'*)  $\Delta$ *mepM* was performed with the pHV30  
371 vector or recombinant plasmids encoding PBP4, PBP7, and AmpH under the control of the  $P_{rhaBAD}$   
372 promoter. Induction of endopeptidase (ED) genes was performed with 0.2% L-rhamnose in the presence  
373 or absence of 16  $\mu$ g/ml ampicillin, 32  $\mu$ g/ml cefsulodin, or 8  $\mu$ g/ml aztreonam. BHI agar plates contained  
374 40  $\mu$ M IPTG and 1% L-arabinose for induction *ycbB* and *relA'*, respectively.

375



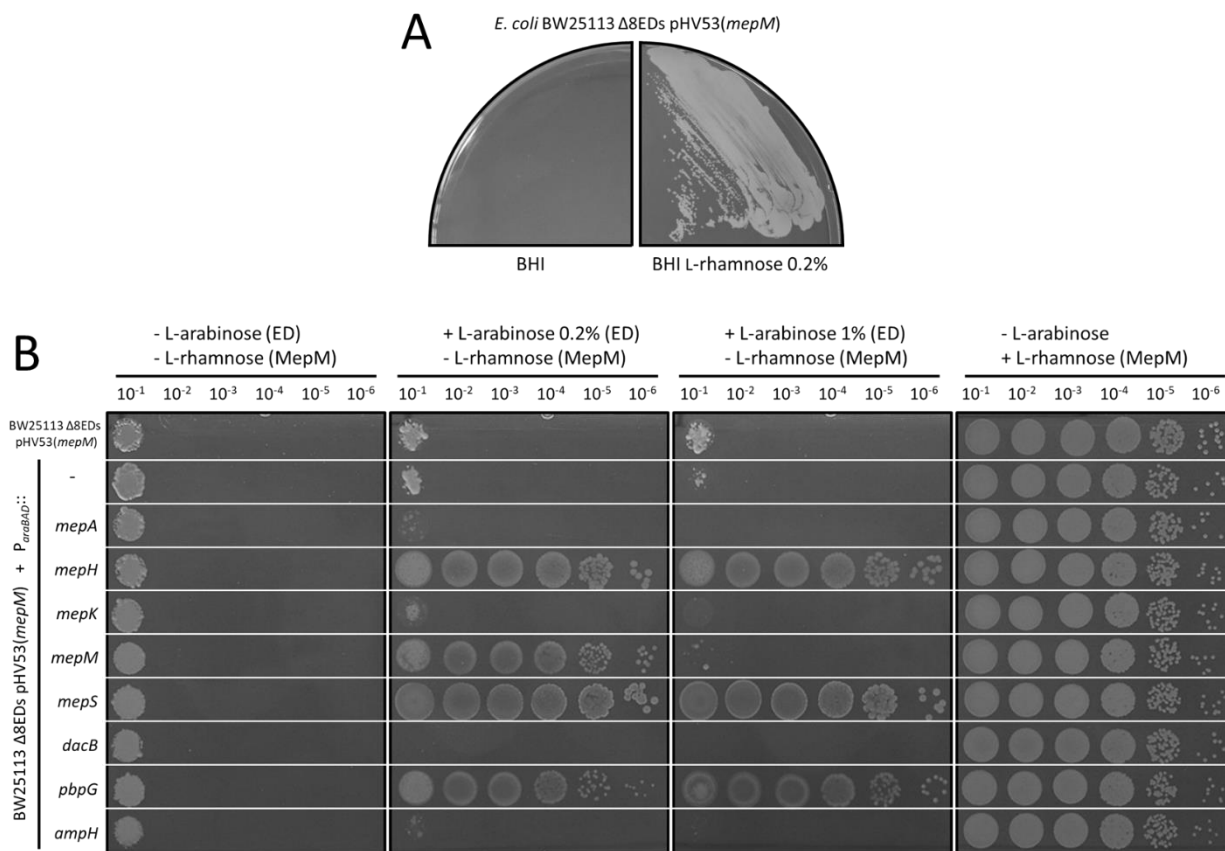
376  
 377 **Figure 7. Hydrolysis of 4→3 and 3→3 cross-links by purified endopeptidases.** Sacculi were incubated with  
 378 lysozyme and purified MepH (A), MepS (B), PBP4 (C), and PBP7 (D). The relative peak areas of Tri-Tri and  
 379 Tri-Tetra containing 3→3 cross-links and that of Tetra-Tri and Tetra-Tetra containing 4→3 cross-links were  
 380 combined. MepH preferentially hydrolyzed dimers containing 4→3 cross-links. MepS hydrolyzed dimers  
 381 containing 4→3 and 3→3 cross-links with similar efficacies. PBP4 and PBP7 only hydrolyzed dimers  
 382 containing 4→3 cross-links. The insets show variations in the relative peak areas of the Tri and Tetra  
 383 monomers. MepH and MepS displayed L,D-carboxypeptidase activity, but not PBP4 and PBP7.

384  
 385 **Minimal complement of endopeptidases required for growth in the context of the formation of**  
 386 **4→3 cross-links by PBPs**

387 Previous analyses based on multiple deletions showed that genes encoding endopeptidases  
 388 belonging to the PBP family (PBP4, PBP7, and AmpH) are collectively dispensable (Denome et al.,  
 389 1999). Independently, deletion of the genes encoding MepH, MepM, and MepS in various  
 390 combinations revealed that at least one of these endopeptidases was essential (Singh et al.,  
 391 2012). Here, we extend these analyses to the full complement of the eight endopeptidase genes.

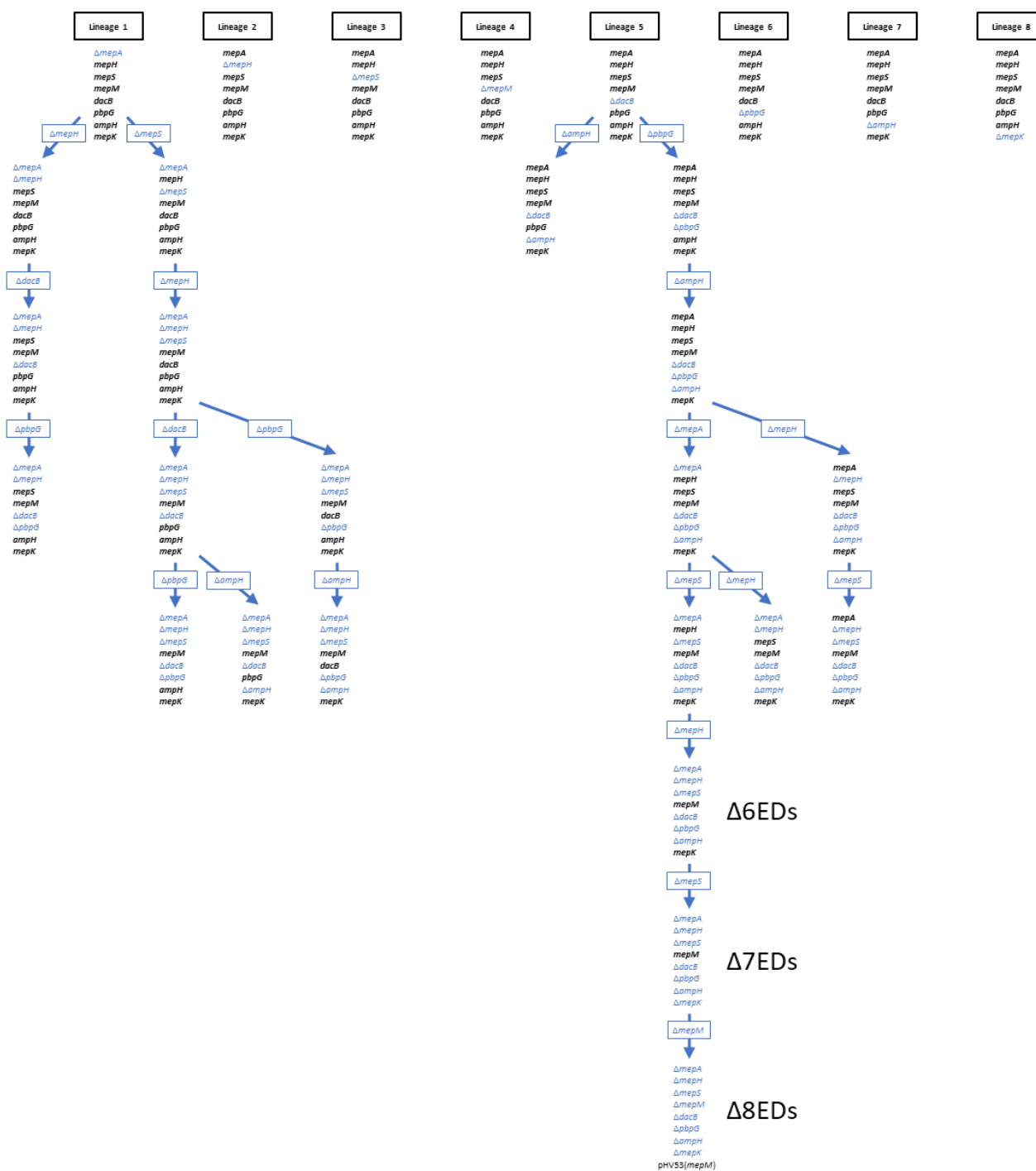
392 Serial deletions of endopeptidase genes were introduced into the chromosome of *E. coli*  
393 BW25113  $\Delta relA$  generating the lineages depicted in supplementary Fig. S4. This approach  
394 culminated in the construction of a viable derivative of BW25113  $\Delta relA$ , designated  $\Delta 7EDs$   
395 (lineage 5 in supplementary Fig. S4), which retained only one of the eight endopeptidase genes  
396 (*mepM*). Thus, MepM alone was necessary and sufficient to support bacterial growth in the  
397 context of the 4 $\rightarrow$ 3 mode of cross-linking.

398 Our next objective was to determine whether deletion of *mepM* could be complemented by  
399 overproduction of other endopeptidases. To address this question, the *mepM* gene was cloned  
400 under the L-rhamnose-inducible promoter of vector pHV30 and introduced into the  $\Delta 7EDs$  strain.  
401 The chromosomal copy of *mepM* was deleted from the resulting strain leading to strain  $\Delta 8EDs$   
402 pHV53(*mepM*), which was dependent upon the presence of L-rhamnose for growth (Fig. 8A). The  
403 plasmids enabling L-arabinose-inducible expression of the eight endopeptidase genes (above)  
404 were introduced in the  $\Delta 8EDs$  pHV53(*mepM*) strain to determine which endopeptidase could  
405 functionally replace MepM (Fig. 8B). Induction by L-arabinose of the genes encoding MepM,  
406 MepH, MepS, and PBP7 suppressed the requirement for L-rhamnose for growth. These results  
407 indicate that a single endopeptidase, MepM, MepH, MepS, or PBP7, is potentially sufficient for  
408 growth in the context of the 4 $\rightarrow$ 3 mode of cross-linking. Except for MepM, this required  
409 overproduction of the enzymes following induction of the  $P_{araBAD}$  promoter of the recombinant  
410 plasmids.



411

412 **Figure 8. Minimal complement of endopeptidases required for growth in the context of the formation**  
 413 **of 4→3 cross-links by PBPs. (A)** BW25113  $\Delta$ 8EDs harboring a plasmid carrying the *mepM* gene under the  
 414 control of the *P<sub>rhaBAD</sub>* L-rhamnose-inducible promoter with the “weak” TIS2 translation initiation signal  
 415 (plasmid pHV53) was grown on BHI agar in the absence or presence of 0.2% L-rhamnose. Growth was  
 416 dependent upon induction of the *mepM* copy carried by pHV53. **(B)** The plating efficiency assay was  
 417 performed with derivatives of BW25113  $\Delta$ 8EDs pHV53(*mepM*) harboring the vector pHV7 or recombinant  
 418 plasmids carrying each of the eight endopeptidase genes under the control of the *P<sub>araBAD</sub>* promoter. In this  
 419 assay, functional replacement of MepM is detected based on growth in media containing 0.2% or 1% L-  
 420 arabinose for expression of the endopeptidase gene carried by vector pHV7, while by-passing the  
 421 requirement for induction of the *mepM* copy of pHV53 by L-rhamnose. Complementation was observed  
 422 with both concentrations of inducer for *mepH*, *mepS*, and *pbpG*. Overproduction of *mepM* encoded by the  
 423 pHV7 derivative in the presence of the high dose of L-arabinose (1%) was lethal. The right panel presents  
 424 the growth control performed in the presence of 0.2% L-rhamnose for induction of the *mepM* copy carried  
 425 by pHV53.



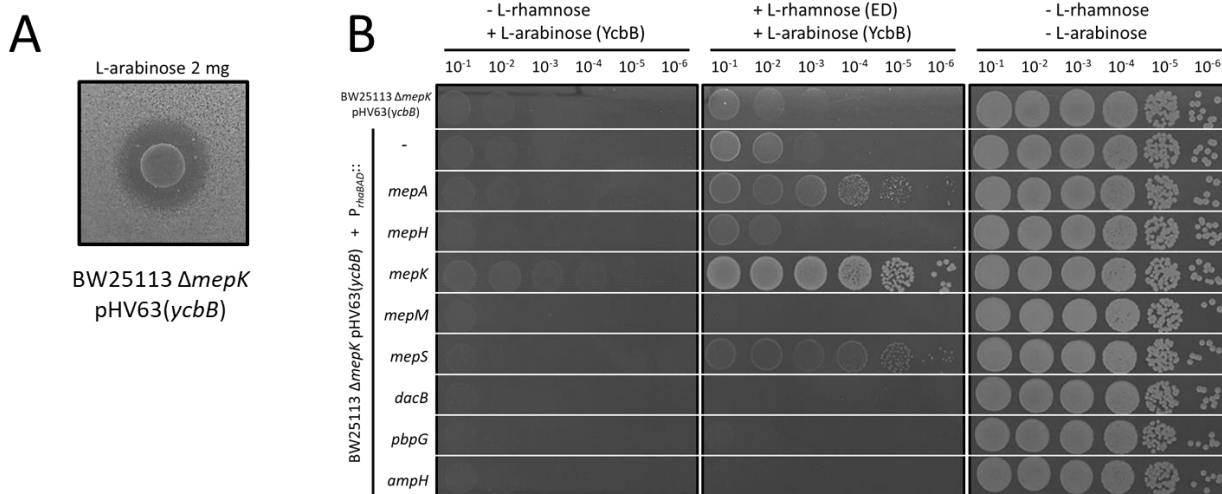
426  
427 **Figure S4. Parallel and serial deletion of endopeptidase genes in *E. coli* BW25113  $\Delta relA$ .** Deletions  
428 indicated in blue were introduced by the procedure of Datsenko and Wanner (Datsenko and Wanner,  
429 2000). The remaining endopeptidase genes are indicated in black. The presence of all deletions was  
430 verified by PCR at each step. The genomes of the strains retaining *mepM* and *mepK* ( $\Delta 6EDs$ ) or only *mepM*  
431 ( $\Delta 7EDs$ ) were re-sequenced and no compensatory mutation was detected.

432

433 **MepA and MepS compensate for the absence of MepK when *ycbB* is induced**



434 The basal production of the YcbB L,D-transpeptidase encoded by plasmid pKT2(*ycbB*) in the  
 435 absence of induction was found to be lethal in a derivative of BW25113 lacking *mepK* (above). To  
 436 investigate the possibility that MepK might be replaced by another endopeptidase, the *ycbB* gene  
 437 was cloned under the control of the  $P_{araBAD}$  promoter of vector pHV7 to obtain a lower level of  
 438 expression of the L,D-transpeptidase gene. The resulting plasmid, pHV63(*ycbB*) was successfully  
 439 introduced into the BW25113  $\Delta mepK$  strain indicating that the basal level of expression of *ycbB*  
 440 in the absence of induction was compatible with the absence of *mepK*. The disk diffusion assay  
 441 revealed a clear zone around the disk containing L-arabinose indicating that induction of *ycbB* in  
 442 the  $\Delta mepK$  background prevented bacterial growth (Fig. 9A). Plasmids for expression of each of  
 443 the eight endopeptidases under the control of the  $P_{rhaBAD}$  promoter (above) were introduced in  
 444 this strain (Fig. 9B). Bacterial growth was observed in conditions of induction of *ycbB* by L-  
 445 arabinose and of genes encoding MepA and MepS by L-rhamnose. This result indicates that the  
 446 essential role of MepK for PG polymerization mediated by the YcbB L,D-transpeptidase was  
 447 bypassed by overproduction of MepA or MepS.  
 448



449  
 450 **Figure 9. Complementation of the *mepK* deletion by plasmids encoding L-rhamnose-inducible copies of**  
 451 **the eight endopeptidase genes. (A)** Induction of *ycbB* under the control of the  $P_{araBAD}$  promoter in  
 452 BW25113  $\Delta mepK$  pHV63(*ycbB*) was studied by the disk diffusion assay. The clear zone around the disk  
 453 containing L-arabinose indicates that production of YcbB inhibited growth. **(B)** Functional  
 454 complementation of the *mepK* deletion of BW25113  $\Delta mepK$  pHV63(*ycbB*) was performed with the pHV30  
 455 vector or recombinant plasmids encoding each of the eight endopeptidases under the control of the  $P_{rhaBAD}$   
 456 promoter. Induction of *ycbB* and of endopeptidase (ED) genes was performed with 0.2% L-arabinose and

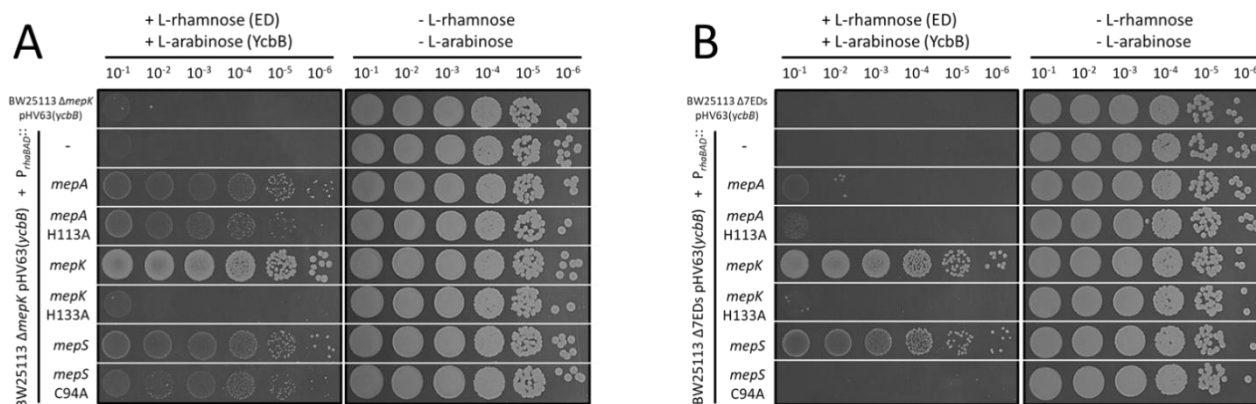


457 1% L-rhamnose, respectively. BHI agar plates contained chloramphenicol (20 µg/ml) to counter-select loss  
458 of pHV63(*ycbB*).

459

#### 460 **Complementation of the *mepK* deletion by catalytically inactivated endopeptidases**

461 Since overproduction of MepK, MepS, and MepA were found to complement the chromosomal  
462 deletion of the *mepK* gene (above, Fig. 9) we focused on these three endopeptidases. Plasmids  
463 encoding catalytically inactive MepK H<sup>133</sup>A, MepS C<sup>94</sup>A, and MepA H<sup>113</sup>A were used to determine  
464 whether the endopeptidase activity of MepK, MepA, and MepS was required to compensate for  
465 the chromosomal deletion of *mepK*. Overproduction of the endopeptidases was tested in the  
466  $\Delta$ *mepK* background (single-deletion mutant retaining all chromosomal endopeptidase genes  
467 except *mepK*) and in the  $\Delta$ 7EDs background (seven-deletion mutant retaining only *mepM*) (Fig.  
468 10). Overproduction of MepK but not MepK H<sup>133</sup>A was essential for growth in both backgrounds  
469 indicating that the catalytic activity of the endopeptidase was essential. Overproduction of MepS  
470 restored growth in both backgrounds but complementation by MepS C<sup>94</sup>A was only observed in  
471 the  $\Delta$ *mepK* single-deletion background. Since the periplasmic protease Prc hydrolyzes MepS  
472 (Singh et al., 2015) overproduction of MepS C<sup>94</sup>A may saturate the protease enabling sufficient  
473 chromosomally-encoded MepS to escape hydrolysis and support growth. Likewise, saturation of  
474 the Prc protease is likely to be responsible for the apparent complementation mediated by  
475 overproduction of MepA and MepA H<sup>113</sup>A since overproduction of these enzymes restored  
476 growth in the  $\Delta$ *mepK* single-deletion background but not in the  $\Delta$ 7EDs background. Together  
477 these results indicate that MepS is the only endopeptidase that can compensate for the absence  
478 of MepK. This required overproduction of MepS. Alternatively, saturation of the Prc protease by  
479 overproduction of MepA, MepA H<sup>113</sup>A, or MepS C<sup>94</sup>A prevented hydrolysis of MepS produced at  
480 a lower level from the native chromosomal *mepS* gene.



481

482 **Figure 10. Complementation of *mepK* deletion with catalytically inactivated endopeptidases.** (A)  
 483 Functional complementation of the *mepK* deletion of BW25113  $\Delta mepK$  pHV63(*ycbB*) was performed with  
 484 the pHV30 vector or recombinant plasmids encoding *mepA*, *mepK*, *mepS* or derivatives encoding  
 485 catalytically inactive endopeptidases under the control of the  $P_{rhaBAD}$  promoter. (B) The complementation  
 486 assay was repeated for BW25113  $\Delta 7EDs$  pHV63(*ycbB*), which was obtained by deletion of all chromosomal  
 487 endopeptidase genes except *mepM*. Induction of *ycbB* and of endopeptidase (ED) genes was performed  
 488 with 0.2% L-arabinose and 1% L-rhamnose, respectively. BHI agar plates contained chloramphenicol (20  
 489  $\mu\text{g/ml}$ ) to counter-select loss of pHV63(*ycbB*).

490

491 **Minimal complement of endopeptidases required for growth in the presence of  $\beta$ -lactams in**  
 492 **the context of the exclusive formation of 3 $\rightarrow$ 3 cross-links by the YcbB L,D-transpeptidase**

493 As previously described (Hugonnet et al., 2016), induction of *relA'* led to mecillinam resistance in  
 494 BW25113(*ycbB*, *relA'*) whereas induction of both *ycbB* and *relA'* was required for ampicillin and  
 495 ceftriaxone resistance (Table 1 and supplementary Fig. S5). Strain BW25113(*ycbB*, *relA'*)  $\Delta 6EDs$   
 496 was also resistant to the three  $\beta$ -lactams upon induction of *ycbB* and *relA'* indicating that 6 of the  
 497 8 endopeptidase genes were dispensable for expression of  $\beta$ -lactam resistance. In contrast to  
 498 BW25113(*ycbB*, *relA'*), the  $\Delta 6EDs$  derivative was resistant to ampicillin and ceftriaxone in the  
 499 absence of induction of *ycbB* by IPTG. The basal level of *ycbB* expression in the absence of  
 500 induction was required for resistance since susceptibility to ampicillin and ceftriaxone was  
 501 observed in the absence of pKT2(*ycbB*). These observations indicate that deletion of 6 of the 8  
 502 endopeptidase genes was associated with a decrease in the level of expression of *ycbB* required  
 503 for  $\beta$ -lactam resistance. In combination with the analysis based on single-gene deletions (Fig. 2B),  
 504 these results show that MepM and MepK are necessary and sufficient for bacterial growth in  
 505 conditions in which YcbB is the only functional transpeptidase.

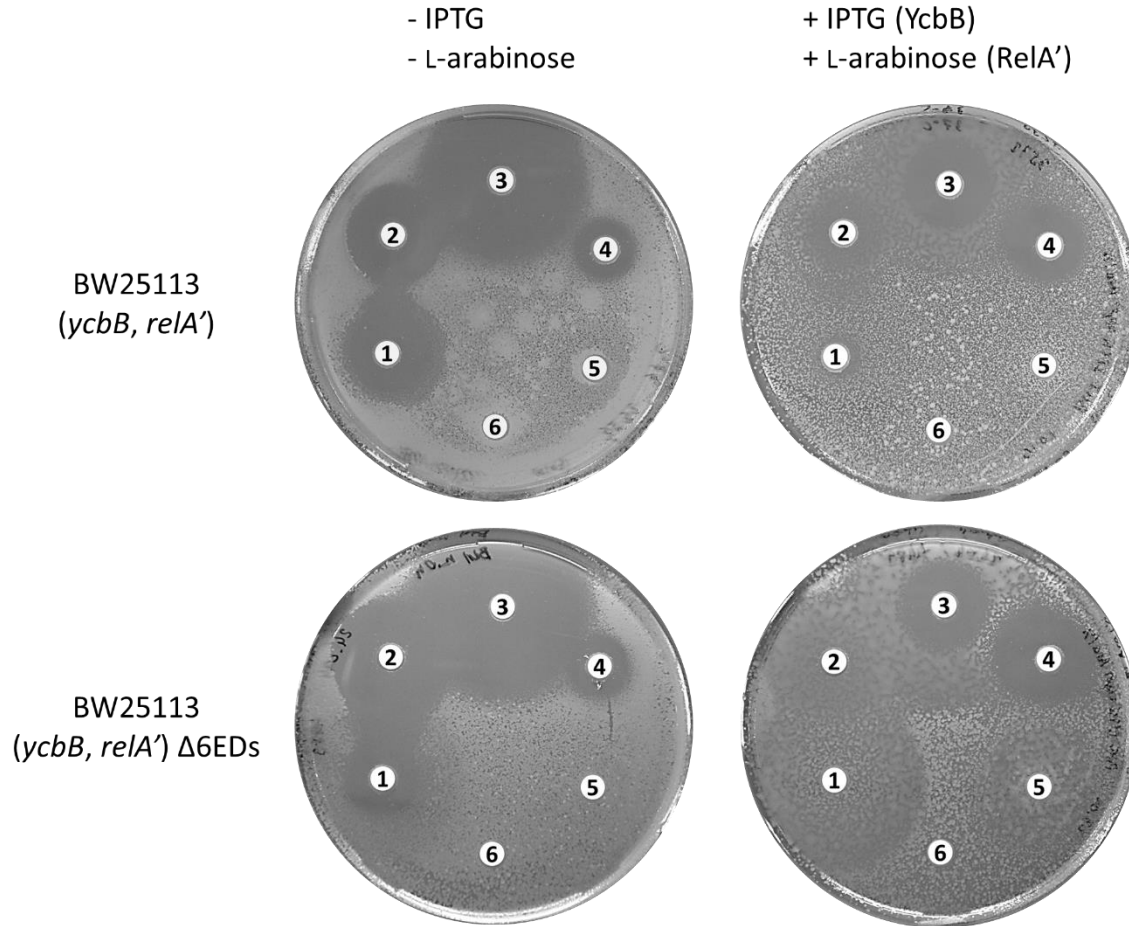
506

**Table 1. YcbB-mediated  $\beta$ -lactam resistance in BW25113 derivatives harboring all endopeptidase genes or only *mepM* and *mepK* ( $\Delta 6ED$ )**

Host	Plasmid	Inducer <sup>b</sup>	Inhibition zones (mm) <sup>a</sup>		
			Mec	Amp	Cro
BW25113 $\Delta relA$					
	pKT2( <i>ycbB</i> ) pKT8( <i>relA'</i> )	None	24	22	38
		IPTG ( <i>ycbB</i> )	28	24	39
		Ara ( <i>relA'</i> )	< 8	24	39
		IPTG + Ara	< 8	< 8	18
BW25113 $\Delta relA$ $\Delta 6EDs$					
	pKT2( <i>ycbB</i> ) pKT8( <i>relA'</i> )	None	17	27	41
		IPTG ( <i>ycbB</i> )	17	28	43
		Ara ( <i>relA'</i> )	< 8	< 8	22
		IPTG + Ara	< 8	< 8	19
BW25113 $\Delta relA$ $\Delta 6EDs$					
	pKT8( <i>relA'</i> )	None	17	27	41
		Ara ( <i>relA'</i> )	< 8	27	41

507 <sup>a</sup> The diameter of inhibition zones was determined by the disk diffusion assay around  
 508 disks containing 10  $\mu$ g mecillinam (Mec), 10  $\mu$ g ampicillin (Amp), or 30  $\mu$ g ceftriaxone  
 509 (Cro). Examples of the original results are presented in supplementary Fig. S5.

510 <sup>b</sup> The *ycbB* and *relA'* genes carried by plasmid pKT2 and pKT8 were induced with 40  
 511  $\mu$ M IPTG and 1% L-arabinose (Ara), respectively.



512  
513 **Figure S5. Antibiotic susceptibility testing by the disk diffusion assay.** Disks contained 10  $\mu$ g mecillinam  
514 (1), 10  $\mu$ g ampicillin (2), 30  $\mu$ g ceftriaxone (3), 30  $\mu$ g tetracycline (4), 30  $\mu$ g chloramphenicol (5), and 30  $\mu$ g  
515 kanamycin (6). Plasmids pKT2(*ycbB*) and pKT8(*relA'*) confer resistance to tetracycline and  
516 chloramphenicol, respectively. Kanamycin resistance is mediated by the Km<sup>R</sup> cassette inserted in place of  
517 *relA*. Induction of *ycbB* and *relA'* was performed with 40  $\mu$ M IPTG and 1% L-arabinose.

518  
519 **Mutations impairing the lytic transglycosylase activity of Slt70 favors YcbB-mediated PG**  
520 **synthesis**

521 Although BW25113(*ycbB*, *relA'*) displays high  $\beta$ -lactam resistance on BHI agar supplemented with  
522 IPTG and L-arabinose, the strain was found to remain susceptible to  $\beta$ -lactams in BHI broth  
523 supplemented with the same inducers. Mutations leading to expression of  $\beta$ -lactam resistance in  
524 liquid medium were sought by selecting mutants derived from *E. coli* BW25113 M1 (Hugonnet et  
525 al., 2016). The latter strain overexpresses *ycbB* carried by plasmid pJEH12(*ycbB*) in response to  
526 induction by IPTG and overproduces the (p)ppGpp alarmone due to impaired expression of the

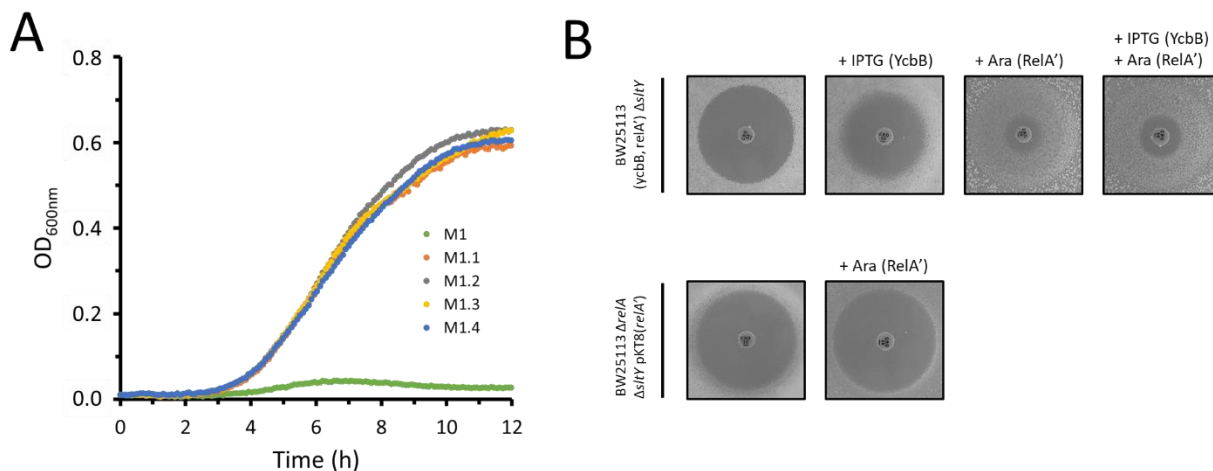
527 isoleucine tRNA synthetase gene *ileS* (Hugonnet et al., 2016). Derivatives of BW25113 M1 were  
 528 selected in BHI broth containing 16 µg/ml ampicillin and 50 µM IPTG. Four independent mutants  
 529 derived from BW25113 M1 (M1.1 to M1.4) were isolated and shown to grow in liquid medium  
 530 supplemented with ampicillin and IPTG (Fig. 11A). Whole genome sequencing revealed single  
 531 mutations all located in the *sItY* gene encoding the SIt70 lytic transglycosylase (Table 2). One of  
 532 the mutants (M1.3) most probably harbored a null allele of *sItY* since a 7-bp deletion introduced  
 533 a frame-shift at the 9<sup>th</sup> codon of the gene. To confirm this conclusion, the *sItY* gene was deleted  
 534 from the chromosome of BW25113(*ycbB*, *relA'*) strain. The resulting strain, BW25113(*ycbB*, *relA'*)  
 535  $\Delta$ *sItY*, was also resistant to ampicillin in liquid medium. Growth of BW25113(*ycbB*, *relA'*)  $\Delta$ *sItY* in  
 536 the presence of ampicillin in liquid medium required the presence of IPTG and L-arabinose  
 537 indicating that overproduction of both the YcbB L,D-transpeptidase and of RelA' remained  
 538 essential for  $\beta$ -lactam resistance. Comparison of the resistance phenotype of BW25113(*ycbB*,  
 539 *relA'*) and its  $\Delta$ *sItY* derivative on BHI agar revealed that overproduction of YcbB upon induction  
 540 by IPTG was dispensable for  $\beta$ -lactam resistance in the absence of SIt70 (Fig 11B). However,  
 541 expression of  $\beta$ -lactam resistance on BHI agar remained dependent upon induction of RelA' by L-  
 542 arabinose and upon the presence of pKT2(*ycbB*). These results indicate that loss of SIt70 was  
 543 essential for expression of YcbB-mediated  $\beta$ -lactam resistance in liquid medium and reduced the  
 544 level of production of the YcbB L,D-transpeptidase required for expression of resistance on solid  
 545 medium. This observation suggests that accumulation of uncross-linked glycan chains in the  
 546 absence of SIt70 may improve the capacity of YcbB to catalyze PG cross-linking accounting for the  
 547 lower level of expression of *ycbB* required for resistance.

**Table 2. Mutations detected in the *sItY* gene of mutants BW25113 M1.1 to M1.4** 548

Mutant	Position	Mutation	Impact <sup>a</sup>	549
M1.1	4,621,672	C→T	Gln <sup>375</sup> stop	550
M1.2	4,622,297	Duplication of AGG CAGGG→CAGGAGGG	Insertion of Gly position 584 (codon GGN)	
M1.3	4,620,572	7-bp deletion CCTGGCGGC→CC	Trp <sup>9</sup> frameshift	
M1.4	4,621,507	C→T	Arg <sup>320</sup> stop	

551 <sup>a</sup> SIt70 comprises 645 amino acid residues.

552



553  
554 **Figure 11. Growth phenotype of *sltY* mutants.** (A) Growth curves of parental strain M1 and mutants M1.1  
555 to M1.4 selected for expression of ampicillin resistance in BHI broth. The growth medium contained 50  
556  $\mu$ M IPTG and 16  $\mu$ g/ml ampicillin. (B) Ceftriaxone-resistance depends upon *ycbB* and *relA'* expression. The  
557 disk diffusion assay was performed with BW25113  $\Delta$ *relA*  $\Delta$ *sltY* harboring pKT2(*ycbB*) and pKT8(*relA'*) or  
558 pKT8(*relA'*) only. Induction was performed with 40  $\mu$ M IPTG and 1% L-arabinose for *ycbB* and *relA'*,  
559 respectively. Disks were loaded with 30  $\mu$ g of ceftriaxone.

560

## 561 DISCUSSION

### 562 Endopeptidases are essential for expansion of sacculi

563 PG polymerization requires a combination of synthetases, the transpeptidases and the  
564 glycosyltransferases, in addition to hydrolases that fulfill two essential roles. Since PG is a net-like  
565 macromolecule completely surrounding the bacterial cell it is beyond any required experimental  
566 demonstration that insertion of new disaccharide-peptide subunits into the growing cell wall  
567 requires cleavage of covalent bonds (Höltje and Heidrich, 2001; Vollmer, 2012). The stress-  
568 bearing PG being present during the entire cell cycle, it is also obvious that PG hydrolases are  
569 required to split daughter cells following completion of septum synthesis (Heidrich et al., 2002).  
570 A portion of these hydrolases generate PG fragments that are imported into the cell and recycled,  
571 a complex pathway that is not essential for growth in laboratory conditions but bears important  
572 roles in (i) minimizing energy costs, (ii) sensing the appropriate balance between synthetic and  
573 hydrolytic activities, which may be altered by  $\beta$ -lactam antibiotics and other toxic agents, and (iii)  
574 avoiding the release of proinflammatory molecules recognized by the host immune system  
575 (Bastos et al., 2020; Johnson et al., 2013). PG hydrolases specifically acting on each of the ten



576 amide, ether, and glycosidic bonds present in the PG polymer have been described and most  
577 cleavage specificities involve multiple enzymes (supplementary Fig. S6A). Enzymes of different  
578 specificities can at least in part compensate for each other, *e.g.* lytic glycosyltransferases and  
579 amidases both contribute to the separation of daughter cells (Heidrich et al., 2002; van  
580 Heijenoort, 2011). In this study, we show that endopeptidases are specifically required for  
581 bacterial growth not only in the context of the formation of 4→3 cross-links by PBPs but also in  
582 the context of the formation of 3→3 cross-links by YcbB (Table 3). We also identify for the first  
583 time the minimum sets of endopeptidases for each mode of PG cross-linking, namely MepM for  
584 4→3 cross-links and MepM plus MepK for 3→3 cross-links. Endopeptidase overproduction  
585 resulting from expression of the genes under the control of heterologous promoters revealed  
586 potential functional redundancies in the endopeptidase families. In particular, overproduction of  
587 MepH, MepS, or PBP7 compensated for the absence of MepM in the context of a 4→3 cross-  
588 linked PG. Overproduction of MepS compensated for the absence of MepM or MepK for growth  
589 with a 3→3 cross-linked PG. Overproduction of MepM prevented growth probably due to  
590 unbalanced synthesis and hydrolysis of PG cross-links (observed for both 4→3 and 3→3 cross-  
591 linked PG). Production of catalytically inactive endopeptidases suggested that MepA and MepS  
592 are negatively regulated by Prc-mediated proteolysis, as previously established for MepS (Lai et  
593 al., 2017; Singh et al., 2015).

594

### 595 **Specificity of purified endopeptidases for 4→3 and 3→3 cross-links**

596 The cleavage specificity of the endopeptidases was determined by mass spectrometry (Fig. 5, 7,  
597 and S2). Endopeptidases of the PBP family were specific to 4→3 cross-links. Endopeptidases  
598 belonging to other families cleaved both 4→3 and 3→3 cross-links with similar efficacies (MepM,  
599 MepS, MepA) or with a preference for 4→3 (MepH) or 3→3 (MepK) cross-links (Fig. 5 and 7)  
600 (Chodisetti and Reddy, 2019; Engel et al., 1992). This is unexpected since 4→3 and 3→3 cross-  
601 links contain amide bonds connecting two R stereo centers (D-Ala<sup>4</sup>→DAP<sup>3</sup>) or an S to an R stereo  
602 center (DAP<sup>3</sup>→DAP<sup>3</sup>), respectively (supplementary Fig. S6A). This could imply that  
603 endopeptidases of the Mep families mainly interact with the acceptor stems of cross-linked  
604 mucopeptides, which are the same for both types of cross-links, whereas endopeptidases of the



605 PBP family interact with a donor tetrapeptide stem only present in 4→3 cross-linked  
606 mucopeptides (supplementary Fig. S6B).

607

### 608 **Integration of endopeptidases into the global regulation of 4→3 and 3→3 PG cross-linking**

609 D,D-carboxypeptidases, which cleave off the terminal residue (D-Ala<sup>5</sup>) of pentapeptide stems, are  
610 thought to negatively control the transpeptidase activity of PBPs since these enzymes require a  
611 pentapeptide donor (Fig. 1). A less studied impact of D,D-carboxypeptidases is the formation of  
612 the essential tetrapeptide donor substrate of the LDTs, except for two publications reporting that  
613 PBP5 and PBP6a are essential for YcbB-mediated β-lactam resistance and for rescue of a defect  
614 in lipopolysaccharide synthesis, respectively (Hugonnet et al., 2016; Morè et al., 2019). Thus, D,D-  
615 carboxypeptidases have crucial roles in controlling the relative contributions of transpeptidases  
616 of the D,D and L,D specificities to PG cross-linking by both decreasing access of PBPs to  
617 pentapeptide stems and increasing access of LDTs to tetrapeptide stems.

618 Endopeptidases participate in the metabolism of PG cross-links in several ways. MepH and  
619 MepS display L,D-carboxypeptidase activity leaving tripeptides as the main (> 80%) end product  
620 of *in vitro* PG hydrolysis (Fig. 7). This activity may negatively control the L,D-transpeptidase activity  
621 of YcbB by hydrolysis of D-Ala<sup>4</sup> thereby preventing access to its tetrapeptide donor. In addition,  
622 hydrolysis of 4→3 cross-linked Tetra→Tetra and Tetra→Tri dimers by the endopeptidases  
623 generates free tetrapeptide stems (Fig. 5 and 7). These tetrapeptide stems can be used as donor  
624 by YcbB for formation of 3→3 cross-links, as demonstrated for the LDTs of *Mycobacterium*  
625 *smegmatis* (Baranowski et al., 2018). In contrast, the D,D-transpeptidase activity of PBPs  
626 exclusively relies on *de novo* synthesis and translocation of pentapeptide-containing precursors  
627 since the D-Ala<sup>5</sup> residue of pentapeptide stems is rapidly cleaved off by D,D-carboxypeptidases if  
628 they are not used for formation of 4→3 cross-links. Thus, YcbB is expected to function as a rescue  
629 enzyme to restore cross-linking in regions of the PG that are compromised by 4→3 or 3→3  
630 endopeptidases. This mechanism was proposed for PG reparation following disassembly of the  
631 lipopolysaccharide export machinery that crosses the PG layer (Morè et al., 2019). The combined  
632 activities of endopeptidases cleaving 4→3 cross-links and of L,D-transpeptidases could contribute

633 to the enrichment in 3→3 cross-links in stationary phase cultures (Pisabarro et al., 1985). In turn,  
634 this enrichment may protect cells from hydrolases active on 4→3 cross-linked PG. Previous  
635 analyses proposed that two L,D-transpeptidases may contribute to the enrichment of PG in 3→3  
636 cross-links, namely YcbB (LdtD), induced by the cell envelope Cpx stress system, and YnhG (LdtE),  
637 expressed under the control of sigma S and induced in stationary phase (Delhaye et al., 2016;  
638 Weber et al., 2005).

639

#### 640 **Participation of YcbB to PG polymerization complexes**

641 PG polymerization is generally thought to be performed by two multiprotein complexes involved  
642 in the expansion of the lateral cell wall (elongasome) and in the formation of the septum  
643 (divisome) (Pazos et al., 2017). Replacement of the D,D-transpeptidase activity of all PBPs by the  
644 L,D-transpeptidase activity of YcbB raises several questions regarding the identity of the partners  
645 of YcbB for the assembly of lateral wall and septum PG, and whether YcbB physically replaces  
646 PBPs in the PG polymerization complexes. Our data support a model in which YcbB functions with  
647 two different sets of partners for lateral wall and septum PG assembly as follows.

648 For the assembly of lateral wall PG, inactivation of the transpeptidase domain of PBP2 by  $\beta$ -  
649 lactams leads to uncoupling of the transglycosylation and transpeptidation reactions, the former  
650 being most probably catalyzed by RodA (Cho et al., 2014; Uehara and Park, 2008). Uncross-linked  
651 glycan chains accumulate in the periplasm and are eventually cleaved by the Slt70 lytic  
652 transglycosylase and recycled. According to the model presented in Fig. 12, and in agreement  
653 with a previous study (Cho et al., 2014), the reactions catalyzed by Slt70 and YcbB occur in  
654 competition implying that YcbB-mediated cross-linking is not coupled to glycan chain  
655 polymerization by RodA. This also implies that YcbB could function in the PG layer in combination  
656 with the MepM endopeptidase known to participate in cell elongation (Banzhaf et al., 2020; Singh  
657 et al., 2012; Truong et al., 2020; Uehara et al., 2009). In agreement with this model, impaired  
658 Slt70 activity had a positive impact on  $\beta$ -lactam resistance mediated by YcbB. This was established  
659 both by the selection of mutations enabling expression of  $\beta$ -lactam resistance in liquid medium,

660 which mapped in the *sltY* gene encoding Slt70 (Table 2) and by the deletion of *sltY*, which lowered  
661 the level of *ycbB* expression required for resistance (Fig. 11).

662 For the assembly of septum PG, YcbB was proposed to cooperate with the glycosyltransferase  
663 activity of Class A PBP1b (Caveney et al., 2019; Hugonnet et al., 2016). In support of this  
664 hypothesis, microscale thermophoresis experiment revealed that purified YcbB interacts with  
665 PBP1b and PBP5 (D,D-carboxypeptidase). Furthermore, the glycosyltransferase activity of PBP1b  
666 is essential for YcbB-mediated  $\beta$ -lactam resistance whereas the combined deletion of class A  
667 PBP1a and PBP1c had no impact. We cannot rule out the possibility that the glycosyltransferase  
668 activity of FtsW also contributes to septum PG polymerization in the presence of  $\beta$ -lactams but  
669 this would require that the inactivation of PBP3 by  $\beta$ -lactams lead to the uncoupling of glycan  
670 chain polymerization and PG cross-linking, as proposed for the RodA-PBP2 complex (see above).  
671 This is not supported by the analyses of PG recycling in conditions of selective inhibition of PBP3  
672 by aztreonam (Uehara and Park, 2008). The endopeptidases involved in septum formation have  
673 not been identified, except for a contribution of PBP4, which has an effect on the timing of  
674 septation (Verheul et al., 2020). MepK is a candidate for this function in 3 $\rightarrow$ 3 cross-linked PG  
675 although this is currently not supported by any experimental evidence and it remains to be seen  
676 if endopeptidases are needed for septum PG synthesis.

677

678

**Table 3. Characteristics of the endopeptidases**

Endopeptidase	<i>In vitro</i> hydrolysis of 4→3 and 3→3 cross-links <sup>c</sup>	Role in the context of the two modes of cross-linking (revealed by endopeptidase overproduction <sup>f</sup> )	
		4→3 cross-links	3→3 cross-links
<b><i>Acyl-serine transferase</i></b>			
PBP4 <sup>a</sup>	4→3	Not essential (None)	Not essential (None)
PBP7 <sup>a</sup>	4→3	Not essential (Compensates for the absence of MepM)	Not essential (None)
AmpH <sup>b</sup>	4→3 <sup>d</sup>	Not essential (None)	Not essential (None)
<b><i>NlpC/P60 peptidase</i></b>			
MepH <sup>a</sup>	4→3 > 3→3 L,D-carboxypeptidase	Not essential (Compensates for the absence of MepM)	Not essential (None)
MepS <sup>a</sup>	4→3 = 3→3 L,D-carboxypeptidase	Not essential (Compensates for the absence of MepM)	Not essential (Compensates for the absence of MepM or MepK) <sup>e</sup>
<b><i>Lysostaphin/M23 peptidase</i></b>			
MepM <sup>a</sup>	4→3 = 3→3	Sufficient (Prevents growth)	Essential (Prevents growth)
<b><i>LAS metallopeptidase</i></b>			
MepA <sup>b</sup>	4→3 = 3→3	Not essential (None)	Not essential (None)
<b><i>M15 peptidase</i></b>			
MepK <sup>b</sup>	4→3 < 3→3	Not essential (None)	Essential (None)

679 <sup>a</sup> Characterized in this study.

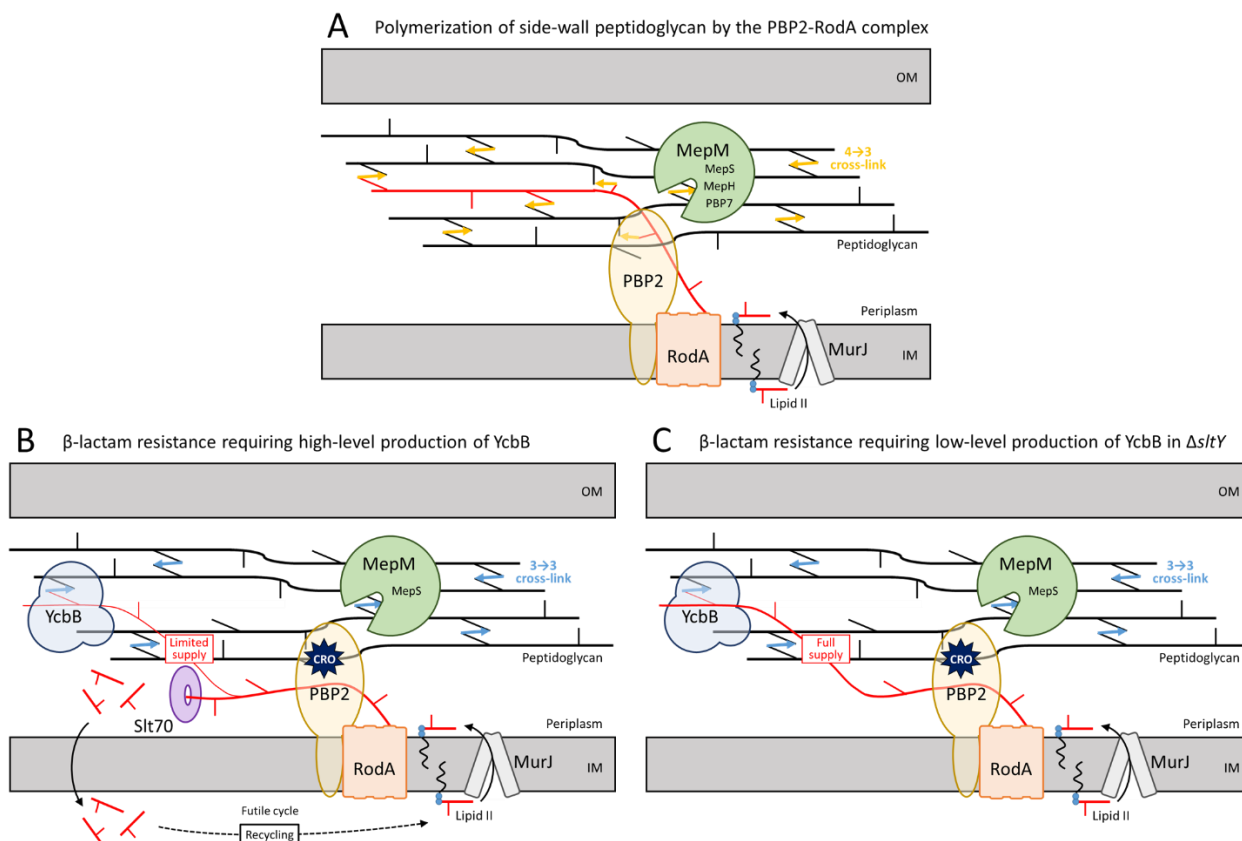
680 <sup>b</sup> Data from the literature (Chodiseti and Reddy, 2019; Engel et al., 1992; Gonzalez-Leiza et al., 2011).

681 <sup>c</sup> MepM, MepS, and MepA cleaved 4→3 and 3→3 cross-links with similar efficacies (4→3 = 3→3). MepH  
682 and MepK displayed a preference for 4→3 cross-links (4→3 > 3→3) or for 3→3 cross-links (4→3 < 3→3),  
683 respectively. L,D-carboxypeptidase, hydrolysis of the DAP<sup>3</sup>-D-Ala<sup>4</sup> amide bond of tetrapeptide stems.

684 <sup>d</sup> Hydrolysis of 3→3 cross-links was not tested.

685 <sup>e</sup> Replacement of both MepM and MepK by MepS was not tested.

686 <sup>f</sup> None, no phenotype associated with endopeptidase overproduction.



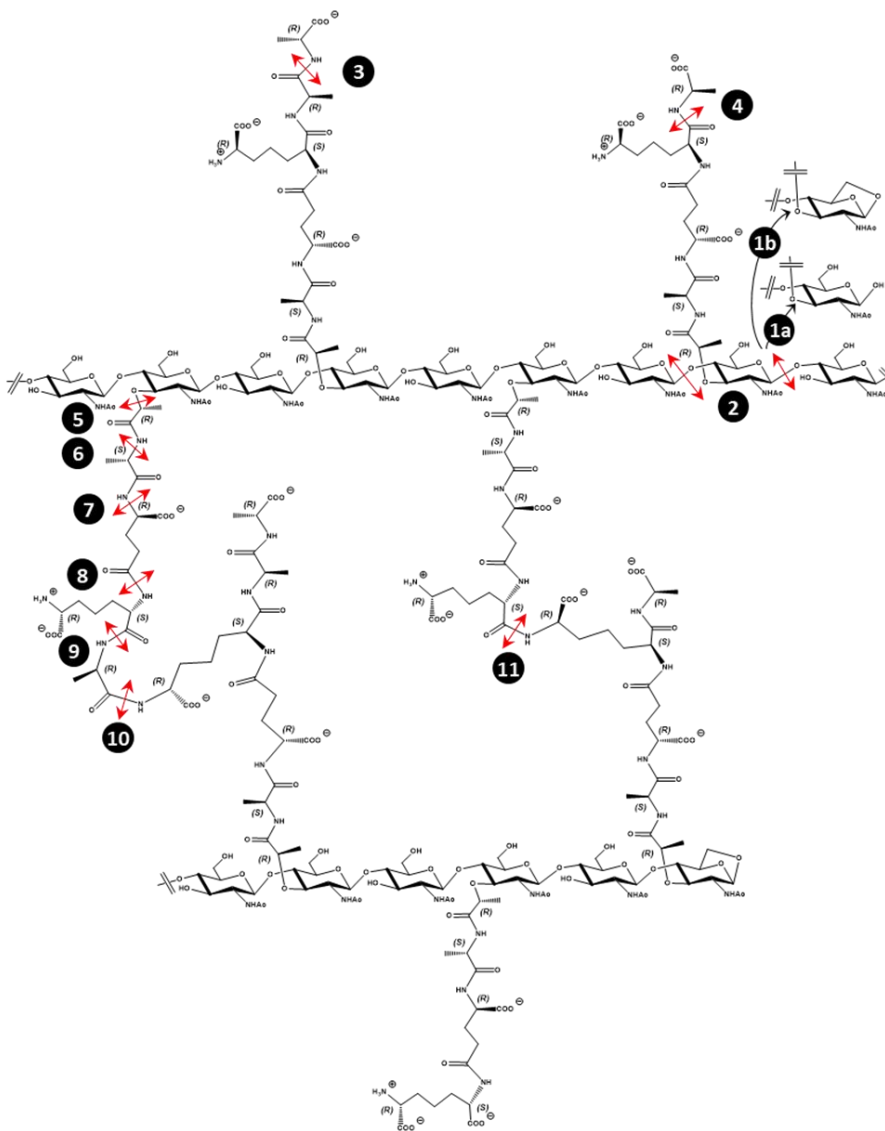
687

688 **Figure 12. Proposed model for polymerization of side wall PG by transpeptidases of the D,D- or L,D-**  
 689 **specificity. (A)** In wild-type cells, the disaccharide pentapeptide subunit linked to the undecaprenyl lipid  
 690 transporter (Lipid II) is translocated to the outer leaflet of the cytoplasmic membrane by MurJ and  
 691 polymerized by the glycosyltransferase and D,D-transpeptidase activities of the PBP2-RodA complex.  
 692 MepM is essential and sufficient for insertion of new material in the PG net, although this endopeptidase  
 693 can be replaced by overproduction of MepH, MepS, or PBP7. **(B)** Inhibition of PBP2 by  $\beta$ -lactams leads to  
 694 the accumulation of uncross-linked glycan chains that are cleaved by the Slt70 lytic transglycosylase. This  
 695 limits the supply of glycan chains for cross-linking by the YcbB L,D-transpeptidase. Under this condition,  
 696 MepM or overproduction of MepS is required for insertion of new glycan strands. **(C)** Deletion of the *slyT*  
 697 gene encoding lytic transglycosylase Slt70 prevents digestion of uncross-linked glycan chains leading to a  
 698 full supply of neo-synthesized glycan chains to YcbB and improved expression of  $\beta$ -lactam resistance. IM,  
 699 inner membrane; OM, outer membrane; CRO, ceftriaxone.

700

**A**

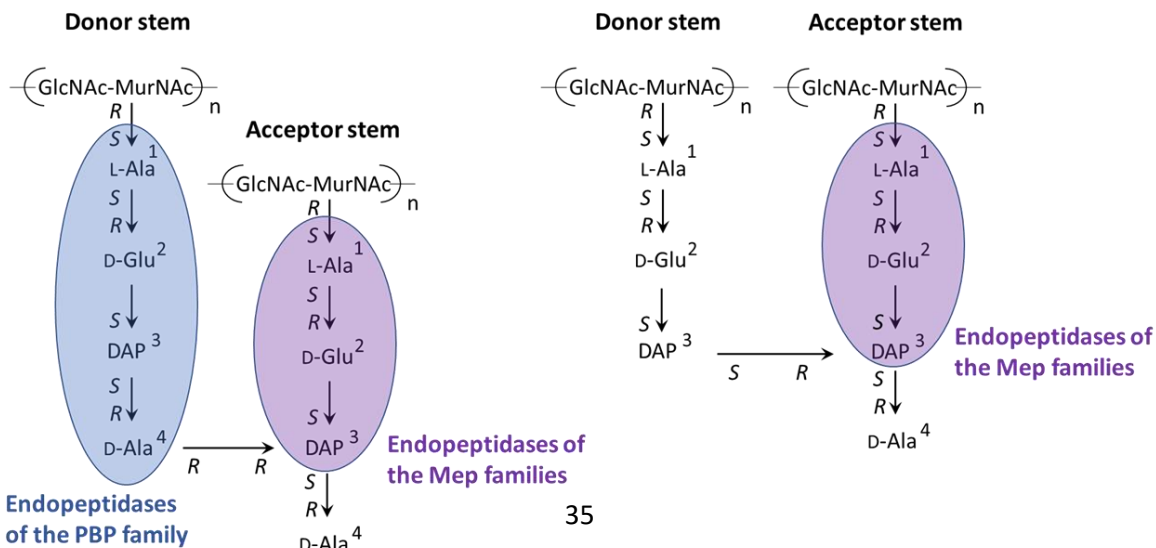
- 1a** Muramidase
- 1b** Lytic transglycosylase
- 2** Glucosaminidase
- 3** D,D-carboxypeptidase
- 4** L,D-carboxypeptidase
- 5** Etherase
- 6** Amidase
- 7** L-Ala-D-iGlu endopeptidase
- 8** D-iGlu-DAP endopeptidase
- 9** DAP-D-Ala endopeptidase
- 10** Endopeptidase 4→3
- 11** Endopeptidase 3→3



**B**

**4→3 cross-linked dimer**

**3→3 cross-linked dimer**



702 **Figure S6. Specificity of PG hydrolases.** (A) Highlight of enzyme stereospecificity. The commonly used  
703 endopeptidase designation was employed in the entire manuscript to refer to the cleavage of internal  
704 bonds although certain enzymes do not cleave peptide bonds connecting the  $\alpha$  amino and carboxyl groups  
705 of two consecutive amino acids and should have been more precisely referred to as amidases. (B).  
706 Recognition of the donor and acceptor stems of dimers by PBP and Mep endopeptidases accounting for  
707 the 4 $\rightarrow$ 3 *versus* 4 $\rightarrow$ 3 plus 3 $\rightarrow$ 3 specificities. According to this model, endopeptidases of the Mep families  
708 cleave both 4 $\rightarrow$ 3 plus 3 $\rightarrow$ 3 cross-links since they interact with the tripeptide portion of the acceptor stem,  
709 which is present in both types of dimers. In contrast, endopeptidases of the PBP families specifically  
710 interact with the tetrapeptide donor stem of 4 $\rightarrow$ 3 cross-linked dimers.

711

## 712 **MATERIALS AND METHODS**

713 **Strains, plasmids, and growth conditions.** All strains were derived from *E. coli* BW25113 (Baba et  
714 al., 2006). The origin and characteristics of plasmids are listed in Supplementary Table S1. Bacteria  
715 were grown in brain heart infusion (BHI; Difco) broth or agar at 37 °C unless otherwise specified.  
716 Liquid cultures were performed with aeration (180 rpm). The growth media were systemically  
717 supplemented with drugs to counter-select plasmid loss (Supplementary Table S1). The same  
718 drugs at the same concentrations were used to select transformants. Kanamycin at 50  $\mu$ g/ml was  
719 used for the Km<sup>R</sup> cassette. Induction of the *lacZYA*, *araBAD*, and *rhaBAD* promoters was  
720 performed with isopropyl  $\beta$ -D-1-thiogalactopyranoside (IPTG, 40 or 50  $\mu$ M), L-arabinose (0.2 or  
721 1%), and L-rhamnose (0.2 or 1%), respectively. Plasmids constructed in this study were obtained  
722 by using NEBuilder HiFi DNA assembly (New England Biolabs) method, unless otherwise specified.

723 Growth curves were obtained in a 96-well plate using an Infinite 200 PRO microplate reader  
724 (TECAN). Briefly, bacteria were grown to the late exponential phase, *i.e.* to an optical density at  
725 600 nm (OD<sub>600</sub>) greater than 1.0 (*ca.* 6 h at 37 °C under agitation). The OD<sub>600</sub> was adjusted to 1.0  
726 and 5  $\mu$ l were inoculated in 195  $\mu$ l of BHI broth supplemented with drugs and inducers, as  
727 specified in the legends to figures. Growth was monitored at 600 nm every 5 min for 12 h at 37  
728 °C with vigorous shaking.

729

730 **Construction of *E. coli* strains carrying gene deletions.** The Keio collection comprises 3,985  
731 mutants obtained by replacement of non-essential genes by a kanamycin resistance (Km<sup>R</sup>)  
732 cassette (Baba et al., 2006). P1 transduction of the Km<sup>R</sup> cassette from selected mutants was used  
733 to introduce deletions of specific genes involved in PG synthesis (Datsenko and Wanner, 2000).  
734 For multiple gene deletions, the Km<sup>R</sup> cassette was removed by the FLT recombinase encoded by



735 plasmid pCP20. The presence of the expected deletions was confirmed by PCR amplification at  
736 each deletion step. Supplementary Fig. S4 shows lineages that have been obtained by parallel  
737 serial deletions.

738 To study the 3→3 mode of cross-linking, plasmid pKT2(*ycbB*) and pKT8(*relA'*) were introduced  
739 into the derivatives of *E. coli* BW25113  $\Delta$ *relA* obtained by deletion of various combinations of  
740 endopeptidase genes. For the sake of simplicity, the latter strains were referred to as  
741 BW25113(*ycbB*, *relA'*) derivatives even though gene deletions preceded the introduction of  
742 pKT2(*ycbB*) and pKT8(*relA'*).

743  
744 **Construction of *E. coli* BW25113  $\Delta$ *relA*  $\Delta$ 8EDs.** The plasmid pHV53(*P*<sub>*rhaBAD*</sub>-TIS2-*mepM*) was  
745 introduced into BW25113  $\Delta$ *relA*  $\Delta$ 7EDs harboring *mepM* as the only chromosomal  
746 endopeptidase-encoding gene. The *mepM* deletion was introduced into BW25113  $\Delta$ *relA*  $\Delta$ 7EDs  
747 pHV53(*P*<sub>*rhaBAD*</sub>-TIS2-*mepM*) in the presence of 0.2% L-rhamnose by P1 transduction as described  
748 above. Growth of the resulting BW25113  $\Delta$ *relA*  $\Delta$ 8EDs pHV53(*P*<sub>*rhaBAD*</sub>-TIS2-*mepM*) strain was  
749 dependent on the induction of the plasmid copy of *mepM* mediated by L-rhamnose.

750  
751 **Mutant selection and whole-genome sequencing.** *E. coli* BW25113 M1 was streaked for isolated  
752 colonies on agar plates containing 10  $\mu$ g/ml tetracycline to counter-select loss of plasmid  
753 pJEH12(*ycbB*). The selection procedure was independently carried out starting with four  
754 independent colonies. Briefly, 5 ml of BHI broth supplemented with 10  $\mu$ g/ml tetracycline and 50  
755  $\mu$ M IPTG were inoculated with a colony. Bacteria were grown overnight with shaking (180 rpm).  
756 A fraction of 1 ml of the culture was inoculated in 250 ml of BHI broth supplemented with 16  
757  $\mu$ g/ml ampicillin and 50  $\mu$ M IPTG. Bacteria were grown overnight with shaking and streaked on  
758 BHI agar containing 16  $\mu$ g/ml ampicillin and 50  $\mu$ M IPTG. A colony was inoculated in 250 ml of BHI  
759 broth supplemented with 16  $\mu$ g/ml ampicillin and 50  $\mu$ M IPTG. Bacteria were grown overnight  
760 with shaking and streaked on BHI agar containing 16  $\mu$ g/ml ampicillin and 50  $\mu$ M IPTG. Five ml of  
761 BHI broth containing 10  $\mu$ g/ml tetracycline was inoculated with a single colony and genomic DNA  
762 was extracted (Wizard DNA extraction kit, Promega). Genomic DNA was sequenced by paired-end

763 joining Illumina (Biomics Platform of the Institut Pasteur, Paris, France). Identification of the  
764 mutations was performed with the *breseq* pipeline (Deatherage and Barrick, 2014).

765  
766 **Plating efficiency assay.** Bacteria were grown to the late exponential phase, *i.e.* to an optical  
767 density at 600 nm (OD<sub>600</sub>) greater than 1.0 (*ca.* 6 h at 37 °C under agitation). The OD<sub>600</sub> was  
768 adjusted to 1.0 and 10-fold dilutions (10<sup>-1</sup> to 10<sup>-6</sup>) were prepared in BHI broth. Ten µl of the  
769 resulting bacterial suspensions were spotted on BHI agar supplemented with inducers and drugs  
770 as indicated in the legend to figures. For the disk diffusion assay, 5 µl of the bacterial suspension  
771 adjusted to an OD<sub>600</sub> of 1.0 were inoculated in 5 ml of water. BHI agar plates were flooded with  
772 the latter suspension, excess liquid was removed, and the plates were kept at room temperature  
773 for 15 min prior to the addition of paper disks containing antibiotics or inducers. Plates were  
774 imaged after 16 h (or 24 h for plates containing ceftriaxone) of incubation at 37 °C.

775  
776 **Purification of endopeptidases.** The *mepM* gene was amplified by PCR and cloned into pET-TEV  
777 between the NdeI and XhoI restriction sites. The fusion protein comprised a 6 x histidine tag, a  
778 TEV protease cleavage site, and residues 41-440 of MepM. The *mepH* and *mepS* genes were  
779 independently amplified by PCR and cloned in frame with *dsbC* into pETMM82 using NEBuilder  
780 HiFi DNA assembly (New England Biolabs). The fusion proteins comprised the DsbC chaperone  
781 (Firczuk and Bochtler, 2007), a 6 x histidine tag, a TEV protease cleavage site, and residues 28-271  
782 of MepH or 25-188 of MepS. The enzymes were produced in *E. coli* BL21(DE3) following induction  
783 by 0.5 mM IPTG for 18 h at 16 °C. The endopeptidases were purified in 50 mM Tris-HCl pH 8.0  
784 from a clarified lysate by nickel affinity chromatography (elution with 0.5 mM imidazole). The  
785 endopeptidases were dialyzed overnight at 4 °C against 50 mM Tris-HCl pH 8.0, 0.5 mM EDTA. N-  
786 terminal tags were cleaved overnight at room temperature following addition of 10 µg of TEV  
787 protease for every mg of protein and DTT at a final concentration of 0.5 mM. MepM, MepH, and  
788 MepS were further purified by size-exclusion chromatography (Superdex 75 HiLoad 26/60, GE  
789 Healthcare) in 50 mM Tris-HCl pH 7.5, 200 mM NaCl.

790 PBP4 was purified from strain BL21(DE3) pET21bΩPBP4Δ1-60 as previously reported  
791 (Banzhaf et al., 2020). Briefly, cells were grown in the presence of 1 mM IPTG for 8 h at 20 °C and

792 then harvested by centrifugation at  $7,500 \times g$ ,  $4^\circ\text{C}$ , 15 min. Cell pellets were resuspended in 50  
793 mM Tris-HCl pH 8.0, 300 mM NaCl, and lysed by sonication. Following centrifugation at  $14,000 \times$   
794  $g$ , 1 h,  $4^\circ\text{C}$ , the NaCl concentration was reduced by stepwise dialysis in a Spectra/Por dialysis  
795 membrane (MWCO 12-14 kDa) against 50 mM Tris-HCl pH 8.5 containing (i) 200 mM NaCl, (ii) 100  
796 mM NaCl, and (iii) 30 mM NaCl. The sample was centrifuged at  $7,500 \times g$ ,  $4^\circ\text{C}$ , 10 min and the  
797 supernatant applied to a 5 ml HiTrap Q HP IEX column in 25 mM Tris-HCl pH 8.5, 30 mM NaCl.  
798 Protein was eluted from the column with a linear gradient from 50 mM Tris-HCl pH 8.5, 100 mM  
799 NaCl, to 25 mM Tris-HCl pH 8.0, 1 M NaCl, over a 100 ml volume. Fractions containing PBP4 were  
800 combined and dialyzed against 10 mM potassium phosphate pH 6.8, 300 mM NaCl. Protein was  
801 applied at 1 ml/min to a 5 ml ceramic hydroxyapatite column (BioRad Bioscale™) in the dialysis  
802 buffer, and a 50 ml linear gradient to 500 mM potassium phosphate pH 6.8, 300 mM NaCl, was  
803 applied. Fractions with PBP4 were dialyzed overnight against 25 mM HEPES-NaOH pH 7.5, 300  
804 mM NaCl, 10% glycerol, and concentrated to *ca.* 5 ml using a Vivaspin concentrator spin column  
805 (Sartorius). The protein sample was applied to a HiLoad 16/600 Superdex 200 column (GE  
806 healthcare) at 1 ml/min and eluted in a linear gradient to 25 mM HEPES-NaOH pH 7.5, 300 mM  
807 NaCl, 10% glycerol. The collected fractions containing PBP4 were combined.

808 PBP7 was purified from strain BL21(DE3) pET28a*QpbbpGΔ1-75* as previously reported  
809 (Banzhaf et al., 2020). Briefly, cells were grown in the presence of 1 mM IPTG for 3 h at  $30^\circ\text{C}$   
810 before being harvested by centrifugation and resuspended in 25 mM Tris-HCl pH 7.5, 500 mM  
811 NaCl, 20 mM imidazole. Following sonication and subsequent centrifugation, the lysate was  
812 applied to a 5 ml HisTrap HP column (GE healthcare) and washed with 4 column volumes of 25  
813 mM Tris-HCl pH 7.5, 500 mM NaCl, 20 mM imidazole. Bound protein was eluted with 25 mM Tris-  
814 HCl pH 7.5, 300 mM NaCl, 400 mM Imidazole. Elution fractions containing PBP7 were combined  
815 and dialyzed overnight against 25 mM HEPES-NaOH pH 7.5, 300 mM NaCl, 10% glycerol, in the  
816 presence of 1 unit/ml of restriction grade thrombin (Novagen) to remove the oligohistidine tag.  
817 The sample was then concentrated to *ca.* 5 ml using a Vivaspin concentrator spin column  
818 (Sartorius) at  $4,500 \times g$ ,  $4^\circ\text{C}$ . The protein sample was applied to a HiLoad 16/600 Superdex 200  
819 column (GE healthcare) at 1 ml/min and eluted in 25 mM HEPES-NaOH pH 7.5, 300 mM NaCl, 10%  
820 glycerol. Elution fractions containing PBP7 were combined.

821 Protein concentrations were determined by the Bio-Rad protein assay using bovine serum  
822 albumin as a standard. Endopeptidases were stored at -80 °C.

823  
824 **Preparation of sacculi.** Bacteria were grown in M9 minimal medium supplemented with 0.1%  
825 glucose at 37 °C for 48 h. Bacteria were harvested by centrifugation and boiled in 4% sodium  
826 dodecyl sulfate (SDS) for 1 h. Sacculi were harvested by centrifugation (20,000 x *g* for 20 min at  
827 20 °C), washed five times with water, and incubated with 100 µg/ml pronase overnight at 37 °C  
828 in 20 mM Tris-HCl pH 7.5. Sacculi were washed five times with water and incubated overnight at  
829 37 °C with 100 µg/ml trypsin in 20 mM sodium phosphate pH 8.0. Sacculi were washed five times  
830 with water, boiled for 5 min, collected by centrifugation, resuspended in water, and stored at -20  
831 °C.

832  
833 **Digestion of sacculi.** Sacculi were digested overnight at 37 °C with 120 µM lysozyme alone or in  
834 association with an endopeptidase in 40 mM Tris-HCl pH 8.0. Insoluble material was removed by  
835 centrifugation and the soluble fraction containing muropeptides was reduced with sodium  
836 borohydride for 1 h in 125 mM borate buffer pH 9.0. The pH of the solution containing the  
837 reduced muropeptides was adjusted to 4.0 with phosphoric acid. Muropeptides were separated  
838 by *rp*HPLC in a C18 column (Hypersil GOLD aQ; 250 x 4.6 mm; 3 µm, Thermoscientific) at a flow  
839 rate of 1 ml/min with a linear gradient (0 to 20%) applied between 10 and 60 min (buffer A, TFA  
840 0.1%; buffer B, acetonitrile 20% TFA 0.1%). Absorbance was monitored at 205 nm and fractions  
841 were collected, lyophilized, and analyzed by mass spectrometry. Mass spectra were obtained on  
842 a Bruker Daltonics maXis high-resolution mass spectrometer (Bremen, Germany) operating in the  
843 positive mode (Analytical Platform of the Muséum National d'Histoire Naturelle, Paris, France).

844

845

**Table S1. Characteristics and origin of the plasmids used in this study**

Plasmid	Characteristics				Origin
<i>Vectors</i>					
pHV6	Tet <sup>R</sup>	<i>P<sub>trc</sub></i>	<i>lacI</i>	<i>oriV</i> CloDF13	This study
pHV7	Cm <sup>R</sup>	<i>P<sub>araBAD</sub></i>	<i>araC</i>	<i>oriV</i> P15a	This study
pHV9	Zeo <sup>R</sup>	<i>P<sub>phIF</sub></i>	<i>phIF</i>	<i>oriV</i> pBR322	This study
pHV30	Zeo <sup>R</sup>	<i>P<sub>rhaBAD</sub></i> TIS1	<i>rhaSR</i>	<i>oriV</i> pSC101	This study

pET-TEV	Km <sup>R</sup> P <sub>T7</sub> <i>lacI</i> <i>oriV</i> ColE1	(Houben et al., 2007)
pETMM82	Km <sup>R</sup> P <sub>T7</sub> <i>dsbC</i> <i>lacI</i> <i>oriV</i> ColE1	(Firczuk and Bochtler, 2007)
<i>Recombinant plasmids for ycbB and relA' expression</i>		
pKT2	pHV6Ω <i>ycbB</i>	(Hugonnet et al., 2016)
pKT8	pHV7Ω <i>relA'</i>	(Hugonnet et al., 2016)
pHV63	pHV7Ω <i>ycbB</i>	This study
<i>Recombinant plasmids for complementation of endopeptidase gene deletions</i>		
pHV10.1	pHV9Ω <i>mepM</i>	This study
pHV10.2	pHV9Ω <i>mepM</i> H <sup>393A</sup>	This study
pHV10.3	pHV9Ω <i>mepM</i> Δ936-1224 (ΔLytM domain)	This study
pHV43.1	pHV30Ω <i>mepA</i>	This study
pHV43.2	pHV30Ω <i>mepA</i> H <sup>113A</sup>	This study
pHV44	pHV30Ω <i>mepH</i>	This study
pHV45.1	pHV30Ω <i>mepK</i>	This study
pHV45.2	pHV30Ω <i>mepK</i> H <sup>133A</sup>	This study
pHV46	pHV30Ω <i>mepM</i>	This study
pHV47.1	pHV30Ω <i>mepS</i>	This study
pHV47.2	pHV30Ω <i>mepS</i> C <sup>94A</sup>	This study
pHV48	pHV30Ω <i>dacB</i>	This study
pHV49	pHV30Ω <i>pbpG</i>	This study
pHV50	pHV30Ω <i>ampH</i>	This study
pHV53	pHV30ΩTIS2- <i>mepM</i>	This study
pHV55	pHV7Ω <i>mepA</i>	This study
pHV56	pHV7Ω <i>mepH</i>	This study
pHV57	pHV7Ω <i>mepK</i>	This study
pHV58	pHV7Ω <i>mepM</i>	This study
pHV59	pHV7Ω <i>mepS</i>	This study
pHV60	pHV7Ω <i>dacB</i>	This study
pHV61	pHV7Ω <i>pbpG</i>	This study
pHV62	pHV7Ω <i>ampH</i>	This study
<i>Recombinant plasmids for protein production</i>		
pET-TEVΩ <i>mepM</i> Δ1-120	Production of MepM Δ1-40	This study
pETMM82Ω <i>mepH</i> Δ1-81	Production of MepH Δ1-27	This study
pETMM82Ω <i>mepS</i> Δ1-72	Production of MepS Δ1-24	This study
pET21bΩ <i>dacB</i> Δ1-60	Production of PBP4 Δ1-20	Banzhaf <i>et al.</i> , 2020
pET28aΩ <i>pbpG</i> Δ1-75	Production of PBP7 Δ1-25	Banzhaf <i>et al.</i> , 2020

846

**Table S2. Characteristics and origin of *E. coli* strains used in this study**

Strain	Characteristics	Origin
BW25113	Δ( <i>araD-araB</i> )567 Δ( <i>rhaD-rhaB</i> )568 Δ <i>lacZ</i> 4787 (::rrnB-3) <i>hsdR514 rph-1</i>	(Baba et al., 2006)
BW25113( <i>ycbB</i> , <i>relA'</i> )	Δ <i>relA</i> derivative of BW25113 harboring pKT2( <i>ycbB</i> ) and pKT8( <i>relA'</i> )	(Hugonnet et al., 2016)
BW25113 M1	Ampicillin resistant derivative of BW25113 pJEH12( <i>ycbB</i> ) harboring a mutation in the 5' UTR region of <i>ileRS</i>	(Hugonnet et al., 2016)
BL21(DE3)	Host for protein production	(Wood, 1966)

847

## 848 **ACKNOWLEDGEMENTS**

849 This work was supported by the French National Research Agency ANR ‘RegOPeps’ (grant ANR-  
850 19-CE44-0007 to JEH). We thank L. Dubost and A. Marie for technical assistance in the collection  
851 of mass spectra. We also thank L. Ma and R. Legendre for technical assistance in genome  
852 sequencing. The Biomix Platform is a member of the ‘France Génomique’ consortium supported  
853 by the French National Research Agency ANR (grant ANR-10-INBS-0009) and IBISA. We also thank  
854 Z. Edoe for proofreading the manuscript.

855

## 856 **COMPETING INTEREST**

857 The authors declare that there is no conflict of interest.

858

## 859 **REFERENCES**

- 860 Baba T, Ara T, Hasegawa M, Takai Y, Okumura Y, Baba M, Datsenko KA, Tomita M, Wanner BL, Mori H.  
861 2006. Construction of *Escherichia coli* K-12 in-frame, single-gene knockout mutants: the Keio  
862 collection. *Mol Syst Biol* **2**. doi:10.1038/msb4100050
- 863 Banzhaf M, Yau HC, Verheul J, Lodge A, Kritikos G, Mateus A, Cordier B, Hov AK, Stein F, Wartel M, Pazos  
864 M, Solovyova AS, Breukink E, van Teeffelen S, Savitski MM, den Blaauwen T, Typas A, Vollmer W.  
865 2020. Outer membrane lipoprotein Nlpl scaffolds peptidoglycan hydrolases within multi-enzyme  
866 complexes in *Escherichia coli*. *EMBO J* **39**. doi:10.15252/emj.2019102246
- 867 Baranowski C, Welsh MA, Sham L-T, Eskandarian HA, Lim HC, Kieser KJ, Wagner JC, McKinney JD, Fantner  
868 GE, Ioerger TR, Walker S, Bernhardt TG, Rubin EJ, Rego EH. 2018. Maturing *Mycobacterium*  
869 *smegmatis* peptidoglycan requires non-canonical crosslinks to maintain shape. *Elife* **7**.  
870 doi:10.7554/eLife.37516
- 871 Bastos PAD, Wheeler R, Boneca IG. 2020. Uptake, recognition and responses to peptidoglycan in the  
872 mammalian host. *FEMS Microbiol Rev* **45**. doi:10.1093/femsre/fuaa044
- 873 Caveney NA, Caballero G, Voedts H, Niciforovic A, Worrall LJ, Vuckovic M, Fonvielle M, Hugonnet J-E,  
874 Arthur M, Strynadka NCJ. 2019. Structural insight into YcbB-mediated beta-lactam resistance in  
875 *Escherichia coli*. *Nat Commun* **10**:1849. doi:10.1038/s41467-019-09507-0
- 876 Cho H, Uehara T, Bernhardt TG. 2014. Beta-Lactam Antibiotics Induce a Lethal Malfunctioning of the  
877 Bacterial Cell Wall Synthesis Machinery. *Cell* **159**:1300–1311. doi:10.1016/j.cell.2014.11.017
- 878 Chodiseti PK, Reddy M. 2019. Peptidoglycan hydrolase of an unusual cross-link cleavage specificity  
879 contributes to bacterial cell wall synthesis. *Proc Natl Acad Sci* **116**:7825–7830.



- 880 doi:10.1073/pnas.1816893116
- 881 Datsenko KA, Wanner BL. 2000. One-step inactivation of chromosomal genes in *Escherichia coli* K-12  
882 using PCR products. *Proc Natl Acad Sci U S A* **97**:6640–6645. doi:10.1073/pnas.120163297
- 883 Deatherage DE, Barrick JE. 2014. Identification of mutations in laboratory-evolved microbes from next-  
884 generation sequencing data using *breseq*. *Methods Mol Biol* **1151**:165–188. doi:10.1007/978-1-  
885 4939-0554-6\_12
- 886 Delhay A, Collet JF, Laloux G. 2016. Fine-tuning of the Cpx envelope stress response is required for cell  
887 wall homeostasis in *Escherichia coli*. *MBio* **7**:47–63. doi:10.1128/mBio.00047-16
- 888 Denome SA, Elf PK, Henderson TA, Nelson DE, Young KD. 1999. *Escherichia coli* mutants lacking all  
889 possible combinations of eight penicillin binding proteins: Viability, characteristics, and implications  
890 for peptidoglycan synthesis. *J Bacteriol* **181**:3981–3993. doi:10.1128/jb.181.13.3981-3993.1999
- 891 Elowitz MB, Leibler S. 2000. A synthetic oscillatory network of transcriptional regulators. *Nature*  
892 **403**:335–8. doi:10.1038/35002125
- 893 Engel H, van Leeuwen AM, Dijkstra A, Keck W. 1992. Enzymatic preparation of 1,6-anhydro-  
894 mucopeptides by immobilized murein hydrolases from *Escherichia coli* fused to staphylococcal  
895 protein A. *Appl Microbiol Biotechnol* **37**:772–783. doi:10.1007/BF00174845
- 896 Firczuk M, Bochtler M. 2007. Mutational analysis of peptidoglycan amidase MepA. *Biochemistry* **46**:120–  
897 128. doi:10.1021/bi0613776
- 898 Glauner B, Holtje J V., Schwarz U. 1988. The composition of the murein of *Escherichia coli*. *J Biol Chem*  
899 **263**:10088–10095.
- 900 Gonzalez-Leiza SM, de Pedro MA, Ayala JA. 2011. AmpH, a Bifunctional DD-Endopeptidase and DD-  
901 Carboxypeptidase of *Escherichia coli*. *J Bacteriol* **193**:6887–6894. doi:10.1128/JB.05764-11
- 902 Hecht A, Glasgow J, Jaschke PR, Bawazer LA, Munson MS, Cochran JR, Endy D, Salit M. 2017.  
903 Measurements of translation initiation from all 64 codons in *E. coli*. *Nucleic Acids Res* **45**:3615–  
904 3626. doi:10.1093/nar/gkx070
- 905 Heidrich C, Ursinus A, Berger J, Schwarz H, Höltje JV. 2002. Effects of multiple deletions of murein  
906 hydrolases on viability, septum cleavage, and sensitivity to large toxic molecules in *Escherichia coli*.  
907 *J Bacteriol* **184**:6093–6099. doi:10.1128/JB.184.22.6093-6099.2002
- 908 Henderson TA, Young KD, Denome SA, Elf PK. 1997. AmpC and AmpH, proteins related to the class C  
909 beta-lactamases, bind penicillin and contribute to the normal morphology of *Escherichia coli*. *J*  
910 *Bacteriol* **179**:6112–21. doi:10.1128/jb.179.19.6112-6121.1997
- 911 Höltje J V, Heidrich C. 2001. Enzymology of elongation and constriction of the murein sacculus of  
912 *Escherichia coli*. *Biochimie* **83**:103–8. doi:10.1016/s0300-9084(00)01226-8
- 913 Houben K, Marion D, Tarbouriech N, Ruigrok RWH, Blanchard L. 2007. Interaction of the C-Terminal  
914 Domains of Sendai Virus N and P Proteins: Comparison of Polymerase-Nucleocapsid Interactions  
915 within the Paramyxovirus Family. *J Virol* **81**:6807–6816. doi:10.1128/jvi.00338-07
- 916 Hugonnet JE, Mengin-Lecreulx D, Monton A, den Blaauwen T, Carbonnelle E, Veckerlé C, Yves VB, van  
917 Nieuwenhze M, Bouchier C, Tu K, Rice LB, Arthur M. 2016. Factors essential for L,D-transpeptidase-  
918 mediated peptidoglycan cross-linking and  $\beta$ -lactam resistance in *Escherichia coli*. *Elife* **5**.

- 919 doi:10.7554/eLife.19469
- 920 Johnson JW, Fisher JF, Mobashery S. 2013. Bacterial cell-wall recycling. *Ann N Y Acad Sci* **1277**:54–75.  
921 doi:10.1111/j.1749-6632.2012.06813.x
- 922 Keck W, Schwarz U. 1979. *Escherichia coli* murein-DD-endopeptidase insensitive to beta-lactam  
923 antibiotics. *J Bacteriol* **139**:770–4.
- 924 Kocaoglu O, Carlson EE. 2015. Profiling of  $\beta$ -lactam selectivity for penicillin-binding proteins in  
925 *Escherichia coli* strain DC2. *Antimicrob Agents Chemother* **59**:2785–2790. doi:10.1128/AAC.04552-  
926 14
- 927 Korat B, Mottl H, Keck W. 1991. Penicillin-binding protein 4 of *Escherichia coli*: molecular cloning of the  
928 *dacB* gene, controlled overexpression, and alterations in murein composition. *Mol Microbiol* **5**:675–  
929 684. doi:10.1111/j.1365-2958.1991.tb00739.x
- 930 Lai GC, Cho H, Bernhardt TG. 2017. The mecillinam resistome reveals a role for peptidoglycan  
931 endopeptidases in stimulating cell wall synthesis in *Escherichia coli*. *PLOS Genet* **13**:e1006934.  
932 doi:10.1371/journal.pgen.1006934
- 933 Magnet S, Dubost L, Marie A, Arthur M, Gutmann L. 2008. Identification of the L,D-Transpeptidases for  
934 Peptidoglycan Cross-Linking in *Escherichia coli*. *J Bacteriol* **190**:4782–4785. doi:10.1128/JB.00025-08
- 935 Mainardi JL, Fourgeaud M, Hugonnet JE, Dubost L, Brouard JP, Ouazzani J, Rice LB, Gutmann L, Arthur M.  
936 2005. A novel peptidoglycan cross-linking enzyme for a  $\beta$ -lactam-resistant transpeptidation  
937 pathway. *J Biol Chem* **280**:38146–38152. doi:10.1074/jbc.M507384200
- 938 Mainardi JL, Villet R, Bugg TD, Mayer C, Arthur M. 2008. Evolution of peptidoglycan biosynthesis under  
939 the selective pressure of antibiotics in Gram-positive bacteria. *FEMS Microbiol Rev*.  
940 doi:10.1111/j.1574-6976.2007.00097.x
- 941 Morè N, Martorana AM, Biboy J, Otten C, Winkle M, Serrano CKG, Montón Silva A, Atkinson L, Yau H,  
942 Breukink E, den Blaauwen T, Vollmer W, Polissi A. 2019. Peptidoglycan Remodeling Enables  
943 *Escherichia coli* To Survive Severe Outer Membrane Assembly Defect. *MBio* **10**.  
944 doi:10.1128/mBio.02729-18
- 945 Pazos M, Peters K. 2019. Peptidoglycan. *Subcellular Biochemistry*. Springer New York. pp. 127–168.  
946 doi:10.1007/978-3-030-18768-2\_5
- 947 Pazos M, Peters K, Vollmer W. 2017. Robust peptidoglycan growth by dynamic and variable multi-protein  
948 complexes. *Curr Opin Microbiol*. doi:10.1016/j.mib.2017.01.006
- 949 Pisabarro AG, De Pedro MA, Vazquez D. 1985. Structural modifications in the peptidoglycan of  
950 *Escherichia coli* associated with changes in the state of growth of the culture. *J Bacteriol* **161**:238–  
951 242. doi:10.1128/jb.161.1.238-242.1985
- 952 Ringquist S, Shinedling S, Barrick D, Green L, Binkley J, Stormo GD, Gold L. 1992. Translation initiation in  
953 *Escherichia coli*: sequences within the ribosome-binding site. *Mol Microbiol* **6**:1219–1229.  
954 doi:10.1111/j.1365-2958.1992.tb01561.x
- 955 Romeis T, Holtje J-V. 1994. Penicillin-binding Protein 7/8 of *Escherichia coli* is a DD-endopeptidase. *Eur J*  
956 *Biochem* **224**:597–604. doi:10.1111/j.1432-1033.1994.00597.x
- 957 Sanders AN, Pavelka MS. 2013. Phenotypic analysis of *Escherichia coli* mutants lacking L,D-

- 958 transpeptidases. *Microbiology* **159**:1842–1852. doi:10.1099/mic.0.069211-0
- 959 Sauvage E, Kerff F, Terrak M, Ayala JA, Charlier P. 2008. The penicillin-binding proteins: Structure and  
960 role in peptidoglycan biosynthesis. *FEMS Microbiol Rev.* doi:10.1111/j.1574-6976.2008.00105.x
- 961 Schreiber G, Metzger S, Aizenman E, Roza S, Cashel M, Glaser G. 1991. Overexpression of the *relA* gene in  
962 *Escherichia coli*. *J Biol Chem* **266**:3760–3767. doi:10.1016/s0021-9258(19)67860-9
- 963 Singh SK, Parveen S, SaiSree L, Reddy M. 2015. Regulated proteolysis of a cross-link–specific  
964 peptidoglycan hydrolase contributes to bacterial morphogenesis. *Proc Natl Acad Sci* **112**:10956–  
965 10961. doi:10.1073/pnas.1507760112
- 966 Singh SK, SaiSree L, Amrutha RN, Reddy M. 2012. Three redundant murein endopeptidases catalyse an  
967 essential cleavage step in peptidoglycan synthesis of *Escherichia coli* K12. *Mol Microbiol* **86**:1036–  
968 1051. doi:10.1111/mmi.12058
- 969 Truong TT, Vettiger A, Bernhardt TG. 2020. Cell division is antagonized by the activity of peptidoglycan  
970 endopeptidases that promote cell elongation. *Mol Microbiol* **114**:966–978. doi:10.1111/mmi.14587
- 971 Turner RD, Vollmer W, Foster SJ. 2014. Different walls for rods and balls: the diversity of peptidoglycan.  
972 *Mol Microbiol* **91**:862–874. doi:10.1111/mmi.12513
- 973 Uehara T, Dinh T, Bernhardt TG. 2009. LytM-domain factors are required for daughter cell separation and  
974 rapid ampicillin-induced lysis in *Escherichia coli*. *J Bacteriol* **191**:5094–5107. doi:10.1128/JB.00505-  
975 09
- 976 Uehara T, Park JT. 2008. Growth of *Escherichia coli*: Significance of peptidoglycan degradation during  
977 elongation and septation. *J Bacteriol* **190**:3914–3922. doi:10.1128/JB.00207-08
- 978 van Heijenoort J. 2011. Peptidoglycan Hydrolases of *Escherichia coli*. *Microbiol Mol Biol Rev* **75**:636–663.  
979 doi:10.1128/mnbr.00022-11
- 980 Vellanoweth RL, Rabinowitz JC. 1992. The influence of ribosome-binding-site elements on translational  
981 efficiency in *Bacillus subtilis* and *Escherichia coli* in vivo. *Mol Microbiol* **6**:1105–1114.  
982 doi:10.1111/j.1365-2958.1992.tb01548.x
- 983 Verheul J, Lodge A, Yau HC, Liu X, Typas A, Banzhaf M, Vollmer W, den T. 2020. Midcell localization of  
984 PBP4 of *Escherichia coli* is essential for the timing of divisome assembly. *bioRxiv*  
985 2020.07.30.230052. doi:10.1101/2020.07.30.230052
- 986 Vollmer W. 2012. Bacterial growth does require peptidoglycan hydrolases. *Mol Microbiol* **86**:1031–1035.  
987 doi:10.1111/mmi.12059
- 988 Weber H, Polen T, Heuveling J, Wendisch VF, Hengge R. 2005. Genome-wide analysis of the general  
989 stress response network in *Escherichia coli*:  $\sigma$ S-dependent genes, promoters, and sigma factor  
990 selectivity. *J Bacteriol* **187**:1591–1603. doi:10.1128/JB.187.5.1591-1603.2005
- 991 Wood WB. 1966. Host specificity of DNA produced by *Escherichia coli*: Bacterial mutations affecting the  
992 restriction and modification of DNA. *J Mol Biol* **16**:118–133. doi:10.1016/S0022-2836(66)80267-X
- 993